THE JOURNAL OF PHYSICAL CHEMISTRY A

Article

pubs.acs.org/JPCA

Hidden Bond Anomalies: The Peculiar Case of the Fluorinated Amine Chalcogenides

Dani Setiawan, Elfi Kraka, and Dieter Cremer*

Computational and Theoretical Chemistry Group (CATCO), Department of Chemistry, Southern Methodist University, 3215 Daniel Avenue, Dallas, Texas 75275-0314, United States

Supporting Information

ABSTRACT: Bond anomalies have been investigated for a set of 53 molecules with either N−F, Ti−P, Cr−H, Pb−C, or Pb−F bonds for which reverse rather than inverse bond length−bond strength relationships have been previously claimed. The intrinsic strength of each bond investigated was determined utilizing the associated local stretching force constant obtained at the CCSD(T)/aug-cc-pVTZ level of theory. For the metal containing molecules, LC-ωPBE calculations with the aug-cc-pVTZ (Cr, Pb) and the 6-31++G(d,p) basis set (Ti) were carried out. For bonds containing a metal atom, any bond anomaly could not be confirmed. Previously reported results were due to ill-defined bond strength descriptors or lacking accuracy. In the case of the fluoro amines, methyl fluoro amines, and the fluoro amine oxides, direct or hidden bond anomalies were detected, which result from two or more opposing electronic effects: a dominant bond shortening effect due to electron withdrawal and a bond weakening due to lone pair repulsion or hybridization defects. Bond anomalies can be disguised by a complex interplay of electronic effects. These *hidden bond anomalies* could be identified in this work for the fluoro amine chalcogenides.

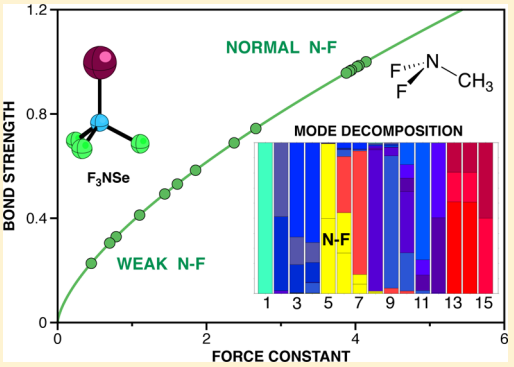

1. INTRODUCTION

One of the tenets of structural chemistry is that the shorter bond is always the stronger bond.[1−5] There is no indisputable theoretical proof for this tenet, which is a reflection of the fact that the chemical bond is a concept rather than an observable quantity.[6−9] Consequently, bond properties such as bond length or bond strength can only be defined within a given model, for example the bond length by considering the nuclei at rest and claiming the distance between them as bond length. This leads immediately to questions in view of the molecular vibrations, the bending of bonds in strained molecules, or the distance at which bonding interactions convert into non-bonding interactions.[7,10,11] Even if these questions might be settled via suitable adjustments of the models used, there is an almost Babylonian confusion if the question of bond strength is addressed. There are static and dynamic bond strength measures depending on whether equilibrium properties or, in a more realistic way, the properties of vibrating molecules are considered.[12,13]

The most popular dynamic bond strength measure is the bond dissociation energy (BDE) or, if experimentally determined, the corresponding enthalpy at 298 K (BDH(298)).[14] This is a highly unreliable measure, as it corresponds to a reaction energy (enthalpy), and as such it depends on the strength of the bond being cleaved *and* the stability of the fragments being formed. The latter are stabilized by an individual relaxation mechanism involving the geometry and the electron density distribution.[8,12]

A frequently used static measure of the bond strength is based on the electron density in the bond region, which should be proportional to the bond strength provided one can define the bond region in a unique way. A solution was offered by Cremer and Gauss[15] who used the density $N(A,B)$ of the zero-flux surface $S(A,B)$ separating bonded atoms A and B to determine the intrinsic bond energy. Utilizing the theory of atoms in molecules,[16] they could describe the bond strength of weakly polar bonds. In general, however the intrinsic bond strength depends also on the polar character of a bond, which cannot be described via $N(A,B)$. A drastic simplification of the Cremer−Gauss approach is achieved by exclusively focusing on the bond critical point $\mathbf{r}_c$ defined as the (3,-1) crossing point (the Hessian of $\rho(\mathbf{r})$ is of rank 3 and signature −1) between the maximum electron density path connecting A and B and the surface $S(A,B)$.[16,17] A single electron density value in the bond region cannot reflect the intrinsic strength of a bond, which depends on the total *bond density*, that is, the distribution of the electron density in the whole bond region.[13] Nevertheless, Gibbs and others[17−19] have shown that in the case of closely related bonds between identical or similar atoms the bond density might be presented by $\rho(\mathbf{r}_c)$, and a simple bond length−bond density relationship might exist. Similarly motivated *static* bond strength parameters have been derived

Received: May 29, 2015
Revised: August 15, 2015
Published: August 17, 2015

DOI: 10.1021/acs.jpca.5b05157
J. Phys. Chem. A 2015, 119, 9541−9556

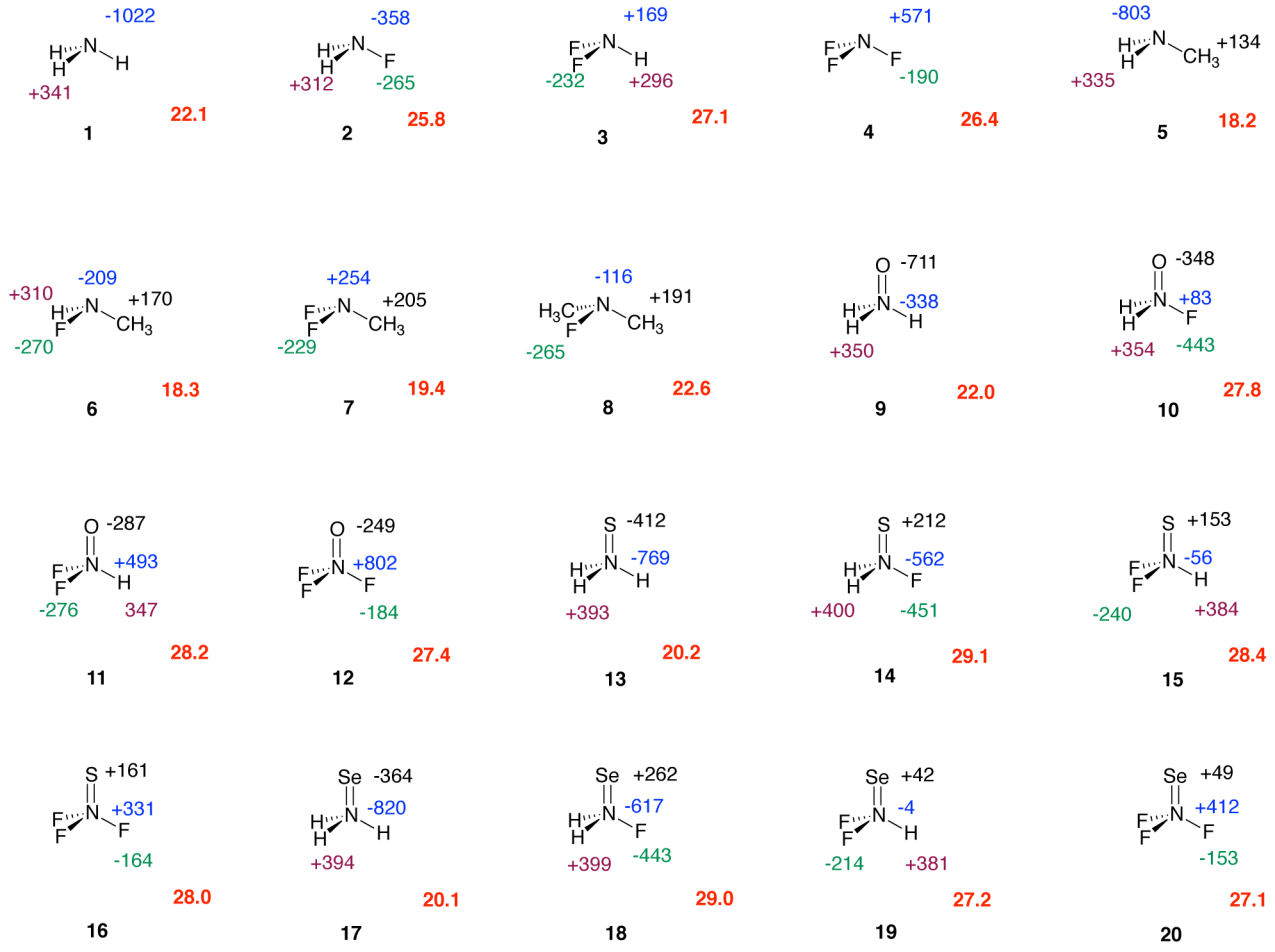

Figure 1. Structures **1**−**20** with CCSD(T)/aug-cc-pVTZ atomic charges (NBO) given in melectron: (blue) central atom; (green) halogen atom; (brown) H atom; (black) other atoms. The bold red numbers give the pyramidalization angle θ.

utilizing, for example, molecular orbitals and their occupation, energy partition methods, density matrices, and electrostatic forces, etc.[3−5,7,9]

In principle, a static description of the bond strength based on either electron density $\rho(\mathbf{r})$ or energy density distribution $H(\mathbf{r})$[7,20,21] might lead to reliable measures provided the problems pointed out above could be solved. Currently, it is easier to access the bond strength via a dynamical model where, instead of a large amplitude motion leading to the cleavage of the bond in question, only infinitesimally small amplitudes are considered, which do not change the electronic structure of the molecule or even break any of its bonds. This leads to the molecular vibrations, which actually cause small changes in the electronic structure.[8] The vibrational properties such as frequencies or force constants are determined for an infinitesimal change in the positions of the atoms in a molecule.[22,23] Hence, the stretching frequency ω_n and stretching force constant k_n of a bond should be suitable quantities to determine the bond strength.[12]

Badger[24,25] showed that for diatomic molecules an *inverse* power relationship between force constant k and bond length R exists. This so-called *Badger Rule*, together with other early observations, laid the basis for the general belief that shorter bonds always imply stronger bonds. However, several recent papers have emphasized that in certain situations the shorter bonds can become the weaker bonds thus indicating a *reverse* rather than inverse bond length−bond strength (BLBS) relationship, for example for the NF bonds in the fluoro amines H_nNF_{3-n} and methyl fluoro amines $(CH_3)_nNF_{3-n}$ with (n = 0−2),[26−31] the A-F bonds in substituted homologues of ethane,[32−34] the O−F bonds in HOF, OF_2, and FNO_2[35−39] or the S−F bonds in the SF_2 dimer,[40,41] Cr−H bonds in chromium dihydrides,[42] or the Ti−P bonds in titanium complexes with phosphines[43,44]

For some of these examples the bond in question connects electronegative atoms possessing electron lone pairs (lp). Therefore, one assumed that lp−lp repulsion might be responsible for a reverse relationship.[13] However, in other cases such as the Pb−P and Pb−C bonds,[45] the Cr−H bonds,[42] or the Ti−P bonds[43,44] lp−lp repulsion does not play any decisive role so that alternative electronic effects had to be invoked to explain the reported reverse BLBS relationships and the resulting *bond anomalies*. Therefore, we investigate in this work several of the systems mentioned in the literature where the focus will be on those claimed bond anomalies that do not involve lp−lp repulsion.

In the following, we will critically evaluate the question whether bond anomalies exist or whether they are just the result of vaguely defined bond strength parameters, experimental or computational shortcomings, or a natural consequence of opposing electronic effects consistent with our general understanding of the chemical bond. For this purpose, we will first (section 2) discuss the computational methods used in this work. The results and the discussion of these

DOI: 10.1021/acs.jpca.5b05157
J. Phys. Chem. A 2015, 119, 9541−9556

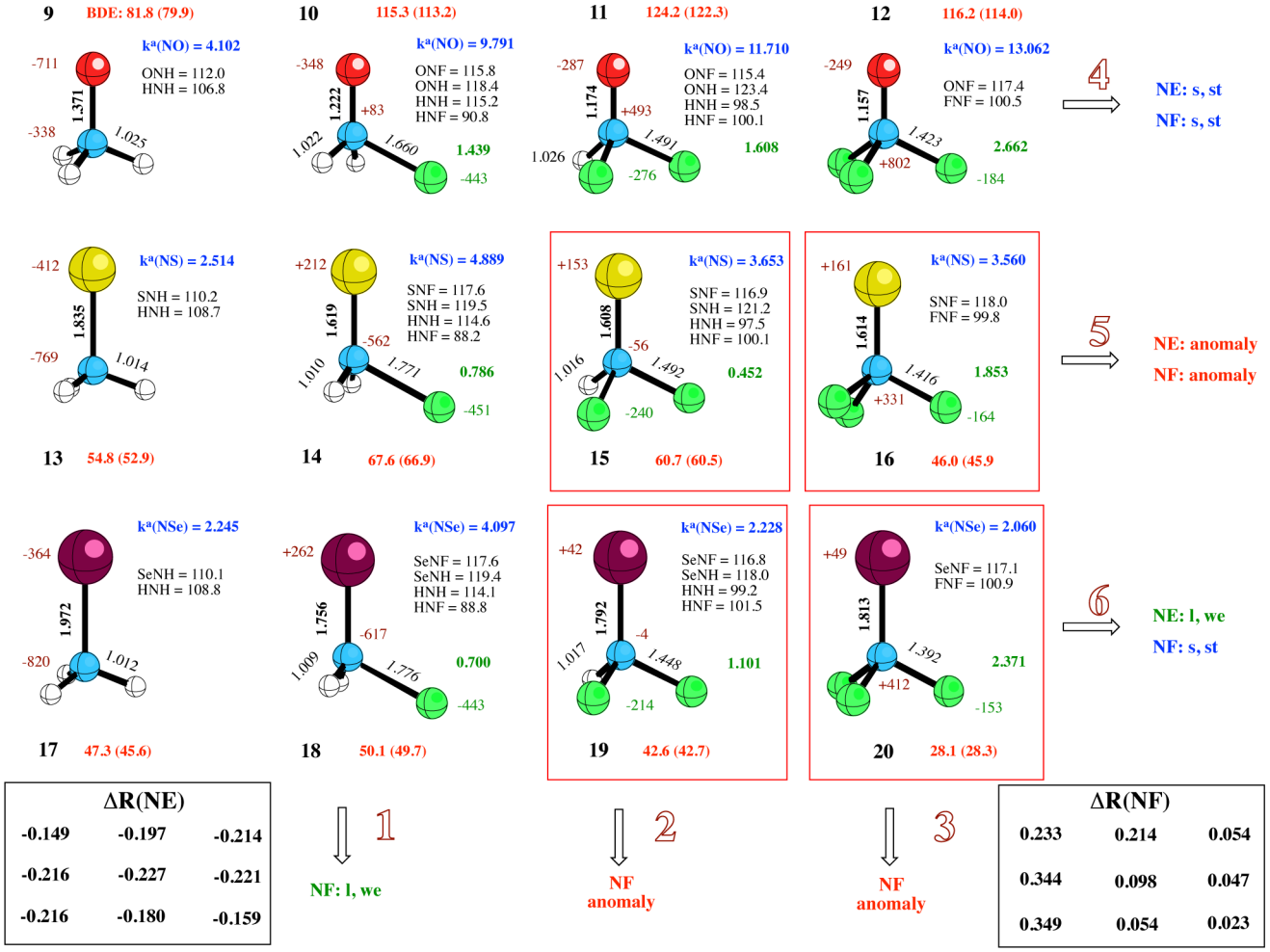

Figure 2. Geometry and bond strength descriptors of the NE (E = O, S, or Se) and NF bonds in fluorinated amine oxides, amine sulfides, and amine selenides **9**−**20** (H, white; N, blue; O, red; F, green; S, yellow; Se, magenta). Bond lengths in Å, bond angles in degrees (black), stretching force constants in mdyn/Å (blue for NE, bold green for NF bond), BDE(NE) and BDH(NE) values (in red) in kcal/mol. Charges of E or N (brown), and F (green) in melectron. Series **1**−**6** (brown outlined numbers) are indicated to lead to NE bond shortening (s), lengthening (l), strengthening (st), weakening (we), or a bond anomaly. Lower left box: NE bond length changes ΔR in Å for **10**−**12**, **14**−**16**, **18**−**20** relative to **9** (first row), **13** (row 2), and **17** (row 3). Lower right box: $\Delta R(NF)$ values relative to **2**−**4**. CCSD(T)/aug-cc-pVTZ calculations.

results will be presented in section 3. Finally, in section 4 the conclusions of this work will be drawn.

2. COMPUTATIONAL METHODS

Normal vibrational modes are delocalized as a result of electronic and kinematic mode−mode coupling.[46] By solving the Wilson equation[22] electronic coupling is eliminated and kinematic coupling remains. In 1998, Konkoli and Cremer showed that elimination of the latter coupling requires the solution of a mass-decoupled Wilson equation, which leads to the local vibrational modes.[46,47] The local modes are driven by an internal coordinate q_n describing the molecular geometry and in this way, they are most useful for the electronic structure analysis. Local modes for curvilinear coordinates or symmetry coordinates can also be defined.[47] Zou and co-workers[48−50] proved that there is a 1:1 relationship between the normal vibrational modes of the Wilson equation and the local vibrational modes obtained by the mass-decoupled Wilson equation: Each of the $N_{vib} = 3N - L$ local vibrational mode frequencies (N, number of atoms; L, number of translations and rotations) of a molecule can be related by an adiabatic connection scheme (ACS) to the N_{vib} normal frequencies. If local modes are driven by $M > N_{vib}$ redundant internal coordinates, $M - N_{vib}$ local vibrational modes relate to normal modes with zero frequencies and therefore are not true local modes. In this way, a unique set of N_{vib} local modes can be identified.[50] In a previous work, the calculation of local mode force constants k_n^a and frequencies ω_n^a as well as the construction of ACS diagrams has been amply described.[48,50−52]

Local mode frequencies can be both measured and calculated although their measurement is limited to specific isotopomers of a target molecule[53−55] or requires special laser techniques in connection with overtone spectroscopy.[56] Local mode force constants, contrary to normal mode force constants, have the advantage of being independent of the choice and the number of coordinates used to describe the molecule in question.[46,47] Since a stretching force constant refers to an infinitesimally small change in the geometry, it does not lead to a change in the electronic structure and, therefore, the local stretching force constant is an excellent probe for the intrinsic strength of a bond.

The usefulness of the local mode description of the intrinsic bond strength[47−49] has been documented by the character-

DOI: 10.1021/acs.jpca.5b05157
J. Phys. Chem. A 2015, 119, 9541−9556

Table 1. Calculated Bond Properties for Molecules 1−32[a]

		B3LYP/aug-cc-pVTZ				CCSD(T)/aug-cc-pVTZ				G4	
no.	molecule (state), sym.	R(AX)	ω^a(AX)	k^a(AX)	n(AX)	R(AX)	ω^a(AX)	k^a(AX)	n(AX)	BDE(AX)	BDH(AX)
					N−F Bonds						
2	$H_2N-F(^1A')$, C_s	1.433	938	4.176	1.000	1.427	934	4.142	1.000	73.10	69.27
3	$H(F)N-F(^1A')$, C_s	1.402	911	3.938	0.964	1.394	923	4.047	0.985	68.30	65.69
4	$F_2N-F(^1A_1)$, C_{3v}	1.379	875	3.637	0.918	1.369	920	4.021	0.981	59.75	58.27
6	$H_3C(H)N-F(^1A)$, C_1	1.443	892	3.782	0.940	1.435	911	3.946	0.968	73.36	70.18
7	$H_3C(F)N-F(^1A')$, C_s	1.413	871	3.605	0.913	1.403	909	3.922	0.964	67.33	65.34
8	$(CH_3)_2N-F(^1A')$, C_s	1.454	854	3.466	0.891	1.436	904	3.878	0.957	73.20	70.55
10	$O=N(H_2)-F(^1A')$, C_s	1.681	497	1.171	0.456	1.660	550	1.439	0.493	51.11	48.67
11	$O=N(H)(F)-F(^1A')$, C_s	1.511	598	1.699	0.574	1.491	582	1.608	0.531	54.03	51.95
12	$O=N(F_2)-F(^1A_1)$, C_{3v}	1.441	719	2.458	0.721	1.424	749	2.662	0.744	53.62	51.79
14	$S=N(H_2)-F(^1A')$, C_s	1.792	348	0.576	0.295	1.771	407	0.786	0.329	32.72	30.84
15	$S=N(H)(F)-F(^1A')$, C_s	1.524	327	0.506	0.272	1.492	308	0.452	0.227	34.15	32.84
16	$S=N(F_2)-F(^1A_1)$, C_{3v}	1.441	549	1.433	0.517	1.416	625	1.853	0.584	36.69	35.85
18	$Se=N(H_2)-F(^1A')$, C_s	1.750	317	0.477	0.262	1.776	384	0.700	0.305	28.66	26.74
19	$Se=N(H)(F)-F(^1A')$, C_s	1.485	336	0.538	0.282	1.448	482	1.101	0.412	31.76	30.46
20	$Se=NF_2-F(^1A_1)$, C_{3v}	1.417	577	1.582	0.549	1.392	707	2.371	0.689	33.23	29.14
					N−H, ON−H, SN−H, SeN−H References						
1	$H_2N-H(^1A_1)$, C_{3v}	1.013	3503	6.796	1.000	1.012	3528	6.894	1.000	114.77	106.73
5	$H_3C(H)N-H(^1A')$, C_s	1.012	3507	6.813	1.001	1.011	3520	6.863	0.999	106.98	99.04
9	$O=N(H_2)-H(^1A_1)$, C_{3v}	1.013	3183	5.610	0.943	1.025	3305	6.052	0.963	59.31	52.81
13	$S=N(H_2)-H(^1A_1)$, C_{3v}	1.016	3468	6.661	0.994	1.014	3520	6.863	0.999	61.63	54.33
17	$Se=N(H_2)-H(^1A_1)$, C_{3v}	1.014	3509	6.822	1.001	1.013	3544	6.958	1.003	67.52	60.16
					NO, NS, NSe						
21	$H_2N-OH(^1A')$, C_s	1.445	942	3.902	0.959	1.443	942	3.905	0.962	69.08	62.98
22	$H_2N-SH(^1A')$, C_s	1.732	699	2.805	0.826	1.730	723	2.995	0.851	70.76	66.14
23	$H_2N-SeH(^1A')$, C_s	1.878	593	2.471	0.811	1.854	628	2.768	0.864	63.10	58.98
24	$HN=O(^1A')$, C_s	1.198	1652	12.005	1.918	1.210	1582	11.007	1.923	167.50	164.71
25	$HN=S(^1A')$, C_s	1.571	1077	6.649	1.406	1.584	1025	6.033	1.359	124.67	122.47
26	$HN=Se(^1A')$, C_s	1.720	879	5.427	1.318	1.725	843	4.986	1.281	106.22	104.31
					PO and AsO Bonds						
27	$H_2P-OH(^1A')$, C_s	1.677	782	3.796	0.912	1.669	808	4.055	0.943	93.22	88.91
28	$H_2As-OH(^1A')$, C_s	1.821	644	3.226	0.814	1.792	692	3.718	0.881	81.24	77.59
29	$HP=O(^1A')$, C_s	1.492	1208	9.076	1.561	1.497	1179	8.633	1.563	184.64	182.98
30	$HAs=O(^1A')$, C_s	1.634	966	7.244	1.341	1.636	951	7.031	1.350	157.57	156.38
					FH Bonds						
31	$F\cdots H\cdots F^-(^1\Sigma_g^+)$, $D_{\infty h}$	1.149	1361	1.044	0.551	1.138	1241	0.868	0.550	43.23	43.96
32	$F-H(^1\Sigma^+)$, $C_{\infty v}$	0.922	4090	9.432	1.102	0.919	4139	9.660	1.101	141.31	136.40

[a]Distance R(AX) in Å, local stretching frequencies ω^a(AX) in cm^{-1}, local AX stretching force constants k^a(AX) in mdyn $Å^{-1}$, and bond strength order n(AX). For molecular structures and NBO charges, see Figure 1.

ization of CC bonds,[47,49,57,58] NN bonds,[12] CO bonds,[59] CX bonds with X = F, Cl, Br, I,[60−64] H-bonding,[51,52,65,66] pnicogen bonding,[67,68] and the characterization of isotopomers.[69] In this work, we will apply the local vibrational mode analysis[46,48,50,70] to a representative test set of 53 molecules, which have been discussed in connection with reverse BLBS relationships or which are needed for reasons of comparison. Molecules **1**−**32** (see Figures 1, 2, and Table 1) contain electron-rich A−X bonds of the type N−F, N−O, N−S, or N−Se, whereas molecules **33**−**53** contain Pb−P, Pb−C, Cr−H, or Ti−P bonds (Figure 3, Table 2), which have been discussed in connection with possible reverse BLBS relationships involving atoms from fourth and higher periods of the periodic table.

Equilibrium geometries and normal vibrational modes of molecules **1**−**32** were calculated at the CCSD(T) level (coupled cluster theory with single (S) and double (D) excitations and a perturbative treatment of triple (T) excitations)[71] using aug-cc-pVTZ basis sets.[72−74] Preliminary calculations were carried out at the DFT (density functional theory) level of theory employing the B3LYP hybrid functional[75−78] with the same basis set. Molecules **33**−**53** containing metals Cr and Pb were calculated with the long-range corrected DFT functional LC-ωPBE[79−81] again employing the aug-cc-pVTZ basis set. In the case of the Ti complexes, Pople's 6-31++G(d,p) basis set[82,83] was used. For molecules containing Pb, the Stuttgart effective core potentials (ECPs) were employed.[84,85] All DFT calculations were carried out using an ultrafine grid[86,87] and tight convergence criteria in the geometry optimizations (forces and displacements $\leq 10^{-6}$ a.u.; changes in the density matrix, $\leq 10^{-8}$) to guarantee a reliable calculation of vibrational properties.

BDE and BDH(298) values were calculated for molecules **1**−**32** with the G4 method.[88] In the case of the Ti−P bonds, BDE and BDH values were calculated at the LC-ωPBE/6-31++G(d,p) level of theory correcting results for basis set superposition errors (BSSEs).[89] All BDEs reported in this

DOI: 10.1021/acs.jpca.5b05157
J. Phys. Chem. A 2015, 119, 9541−9556

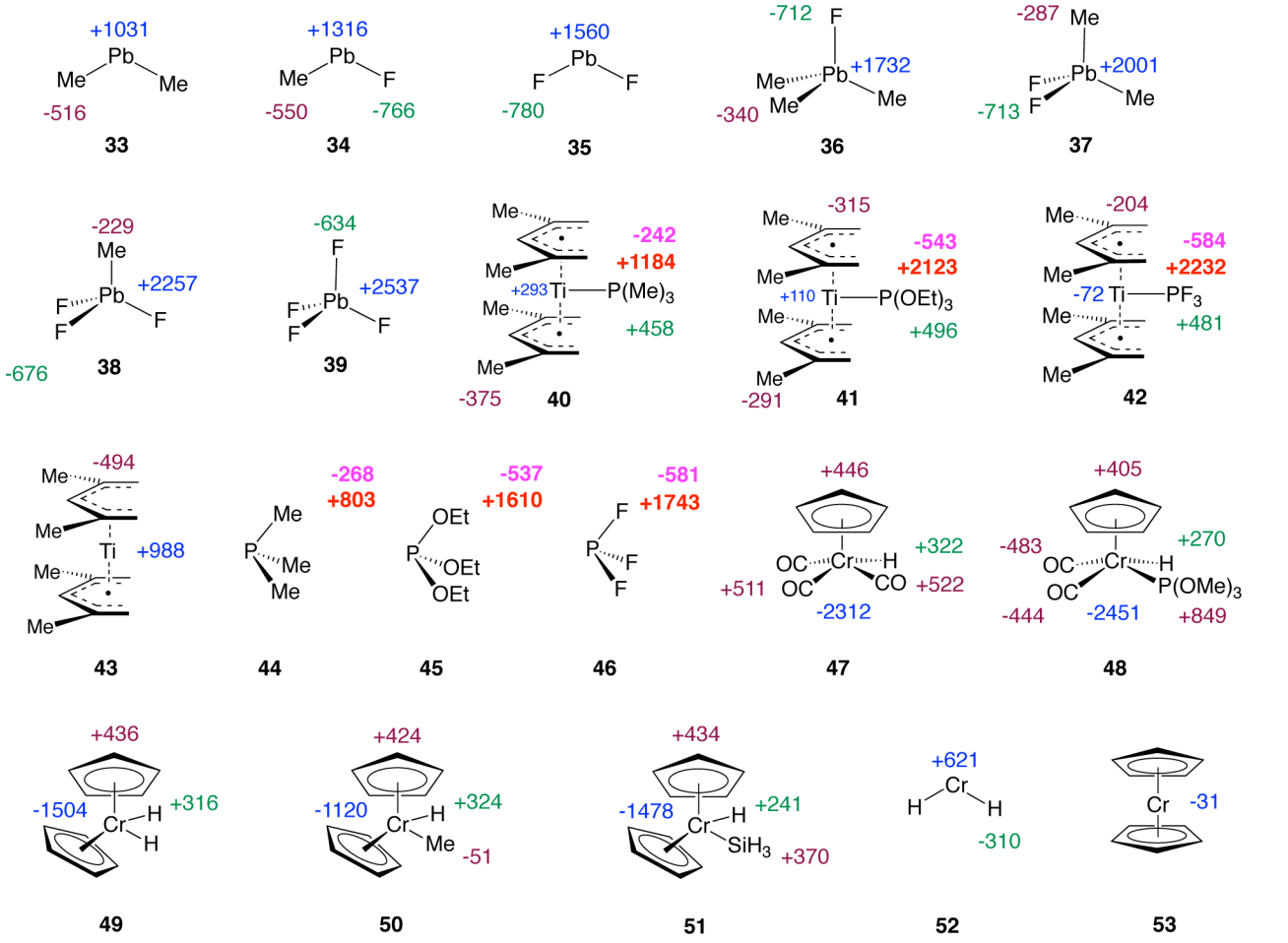

Figure 3. Molecules **33**−**53**. Atomic NBO charges according to LC-ωPBE/aug-cc-pVTZ (Pb, Cr) or LC-ωPBE/6-31++G(d,p) calculations (Ti) are given in melectron: (blue) metal atom; (green) H or halogen atom; (brown) C system; (red) P atom; (purple) phosphine.

work do not include zero-point energies because only the electronic factors influencing their magnitude will be considered. NBO (natural bond orbital) charges[90,91] were determined at the CCSD(T)/aug-cc-pVTZ level (**1**−**33**), at the B3LYP/aug-cc-pVTZ (**1**−**33**), and at the LC-ωPBE level with either the aug-cc-pVTZ or 6-31++G(d,p) basis set (**34**−**53**).

Many of the molecules considered in this work adopt a pyramidal structure where the degree of pyramidalization plays an important role in the discussion. The latter was measured by determining for an AH_nX_m molecule that normal vector which forms with the three AH or AX bond vectors one and the same angle α. The pyramidalization angles were defined as $\theta = \alpha - 90$ so that the planar form of AH_nX_m is identified by $\theta = 0°$.

Intrinsic bond strengths were compared by using the stretching force constants k^a(AZ). To simplify the comparison of force constants, the k^a values were used to derive relative bond strength orders (BSOs) n. The relative BSO n(AX) was calculated by utilizing the extended Badger rule,[12,31] according to which n is related to the local stretching force constant k^a by a power relationship $n = a(k)^b$. The constants a and b are determined with the help of two reference values and the requirement that for a zero force constant n becomes zero. As reference molecules hydroxylamine (**21**; n(NO) = 1.0) and nitroxyl (**24**; n(NO) = 2.0) were used. At the CCSD(T) level, a = 0.402 and b = 0.669 were obtained, and at the DFT level a = 0.432; b = 0.617 were obtained. The resulting equations were used for all bonds investigated in this work. However, for each type of bond A−X investigated, the BSO values were rescaled by introducing additional reference molecules. For example, the BSO values of the NF bonds were scaled by setting the BSO of the N−F bond of **2** to 1.0, and those of the NS (NSe) bonds by using the single bond in H_2N−SH (H_2N−SeH) as reference for n = 1.0.

The BSO values of A−H bonds were calculated from the local stretching force constants by using the FH bonds in $F\cdots H\cdots F^-$ (**31**; n(FH) = 0.5) and HF (**32**; n = 1.0) as suitable reference (CCSD(T): a = 0.521, b = 0.288. B3LYP: a = 0.505, b = 0.306) and, then scaling the resulting $n = f(k^a)$ relationship with the help of reference molecules AH_3. Also, the FH relationship was extended to Cr−H bonds by recalculating it at the LC-ωPBE/aug-cc-pVTZ level of theory. The corresponding k^a(FH) values for **31** and **32** are 1.006 and 9.609 mdyn/Å, respectively. This led to a = 0.499 and b = 0.307. The BSO value of the Cr-dihydride **49** was set to 1.0 to rescale calculated BSO values for Cr−H bonds.

This approach was tested: (i) by calculating the relative BSO values of reference molecules with formal double bonds N═S, N═Se (**25**; **26**) and (ii) single bonds P−O, As−O (**27**; **28**) with formal double bonds P═O, As═O (**29**; **30**). Then the ratio of the BSO values were compared with those of the corresponding BDE values. In all cases, reasonable BSO values were obtained, which qualitatively changed parallel to the calculated BDE values for these bonds (Table 1).

DOI: 10.1021/acs.jpca.5b05157
J. Phys. Chem. A 2015, 119, 9541−9556

Table 2. Calculated Bond Properties for Molecules 33−53[a]

no.	molecule	bond type[b]	R(MA)	k^a(MA)	ω^a(MA)
34	$Pb(CH_3)F$	Pb−F	2.066	2.730	515.9
35	PbF_2	Pb−F	2.045	2.946	535.9
36	$Pb(CH_3)_3F$	Pb−F	2.059	2.765	519.2
37	$Pb(CH_3)_2F_2$	Pb−F	2.039	2.938	535.2
38	$Pb(CH_3)F_3$	Pb−F	1.998	3.397	575.5
39	PbF_4	Pb−F	1.972	3.929	618.9
33	$Pb(CH_3)_2$	Pb−C	2.253	1.780	516.0
34	$Pb(CH_3)F$	Pb−C	2.234	1.863	528.0
36	$Pb(CH_3)_3F$	Pb−C	2.177	2.208	574.8
37	$Pb(CH_3)_2F_2$	Pb−C	2.144	2.347	592.5
38	$Pb(CH_3)F_3$	Pb−C	2.141	2.299	586.5
40	$Ti(\eta^5\text{-}2,4\text{-}C_7H_{11})_2P(Me)_3$	Ti−P	2.521	0.940	291.1
41	$Ti(\eta^5\text{-}2,4\text{-}C_7H_{11})_2P(OEt)_3$	Ti−P	2.416	1.124	318.4
42	$Ti(\eta^5\text{-}2,4\text{-}C_7H_{11})_2PF_3$	Ti−P	2.293	1.753	397.6
40	$Ti(\eta^5\text{-}2,4\text{-}C_7H_{11})_2P(Me)_3$	*Ti*···*X*	1.756	0.941	244.7
41	$Ti(\eta^5\text{-}2,4\text{-}C_7H_{11})_2P(OEt)_3$	*Ti*···*X*	1.753	1.288	286.3
42	$Ti(\eta^5\text{-}2,4\text{-}C_7H_{11})_2PF_3$	*Ti*···*X*	1.743	1.301	287.9
43	$Ti(\eta^5\text{-}2,4\text{-}C_7H_{11})_2$	*Ti*···*X*	1.888	1.054	259.1
47	$Cr(H)(\eta^5\text{-}Cp)(CO)_3$	Cr−H	1.565	2.245	1963.4
48	$Cr(H)(\eta^5\text{-}Cp)(CO)_2P(OMe)_3$	Cr−H	1.576	2.151	1921.8
49	$Cr(H)_2(\eta^5\text{-}Cp)_2$	Cr−H	1.530	2.404	2031.4
50	$Cr(H)(\eta^5\text{-}Cp)_2Me$	Cr−H	1.517	2.468	2058.2
51	$Cr(H)(\eta^5\text{-}Cp)_2SiH_3$	Cr−H	1.567	2.025	1864.6
52	$Cr(H)_2$	Cr−H	1.594	1.997	1851.5
47	$Cr(H)(\eta^5\text{-}Cp)(CO)_3$	*Cr*···*X*	1.802	3.389	454.6
48	$Cr(H)(\eta^5\text{-}Cp)(CO)_2P(OMe)_3$	*Cr*···*X*	1.802	3.335	450.9
49	$Cr(H)_2(\eta^5\text{-}Cp)_2$	*Cr*···*X*	1.760	3.446	458.3
50	$Cr(H)(\eta^5\text{-}Cp)_2Me$	*Cr*···*X*	1.796	2.855	417.2
51	$Cr(H)(\eta^5\text{-}Cp)_2SiH_3$	*Cr*···*X*	1.775	3.434	457.6
53	$Cr(H)(\eta^5\text{-}Cp)_2$	*Cr*···*X*	1.781	2.702	405.9

[a]Distance R(MA) in Å, local stretching frequencies ω^a(MA) in cm^{-1}, and local MA stretching force constants k^a(MA) in mdyn $Å^{-1}$. For molecular structures and NBO charges, see Figure 3. [b]X is the geometrical center of the pentadienyl unit (Ti complexes) or the Cp ring (Cr complexes). LC-ωPBE/aug-cc-pVTZ (Pb, Cr) and LC-ωPBE/6-31++G(d,p) calculations (Ti).

The local vibrational modes[46] were calculated and analyzed with the program package COLOGNE2015.[92] For the CCSD(T) calculations, the program CFOUR[93,94] was used, and for the DFT calculations, Gaussian 09 was used.[95]

3. RESULTS AND DISCUSSION

In Table 1, AX bond properties of compounds **1**−**32** (compare with Figure 1) calculated at the B3LYP/aug-cc-pVTZ and CCSD(T)/aug-cc-pVTZ levels of theory are listed. These comprise the distance R(AX) for A = N and X = F and H, the local stretching frequency ω^a(AX) and force constant k^a(AX), the relative BSO values n(AX), as well as BDE(AX) and BDH(AX) values. NBO charges calculated at the CCSD(T) level are given in Figure 1 for molecules **1**−**20**. Figure 2 summarizes the corresponding data for the NE bonds in molecules **9**−**20**. Figure 4 gives the BSO relationship for all NF bonds investigated in this work. In Table 2, MA bond properties of compounds **33**−**53** calculated at the LC-ωPBE level of theory are listed, comprising the distances R(MA), (M = Pb, Cr, and Ti; A = C, P, H, and F), the local stretching frequencies ω^a(MA), and force constants k^a(MA). Figure 3 gives a summary of the corresponding NBO charges.

BLBS Relationships for NF Bonds. The NF bond anomaly was discussed by several authors on the basis of vaguely determined bond strength descriptors (see below).[27−30] Cremer and Kraka[13] verified the NF bond anomaly by utilizing for the first time local NF stretching force constants derived from low level DFT vibrational modes

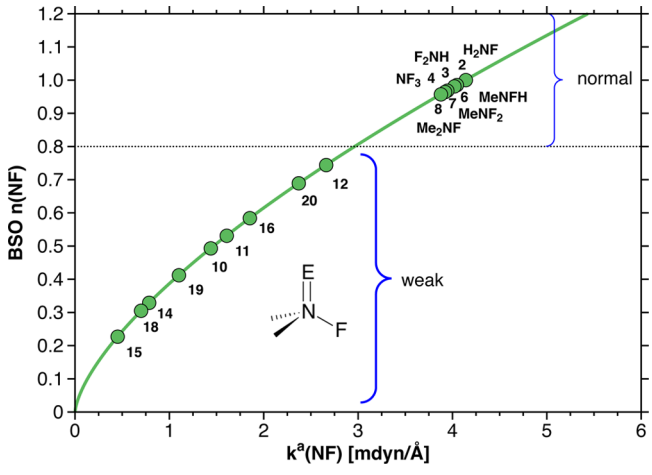

Figure 4. Relative BSO values n(NF) given as a function of the corresponding local NF stretching force constants k^a(NF) according to CCSD(T)/aug-cc-pVTZ calculations. E = O, S, or Se.

DOI: 10.1021/acs.jpca.5b05157
J. Phys. Chem. A 2015, 119, 9541−9556

(B3LYP/6-31G(d,p)) as quantitative bond strength descriptors. Their results are scrutinized and confirmed in this work by using the more reliable CCSD(T) vibrational modes in connection with a larger basis set containing diffuse functions. Figure 5 reveals that all NF bonds investigated in this work

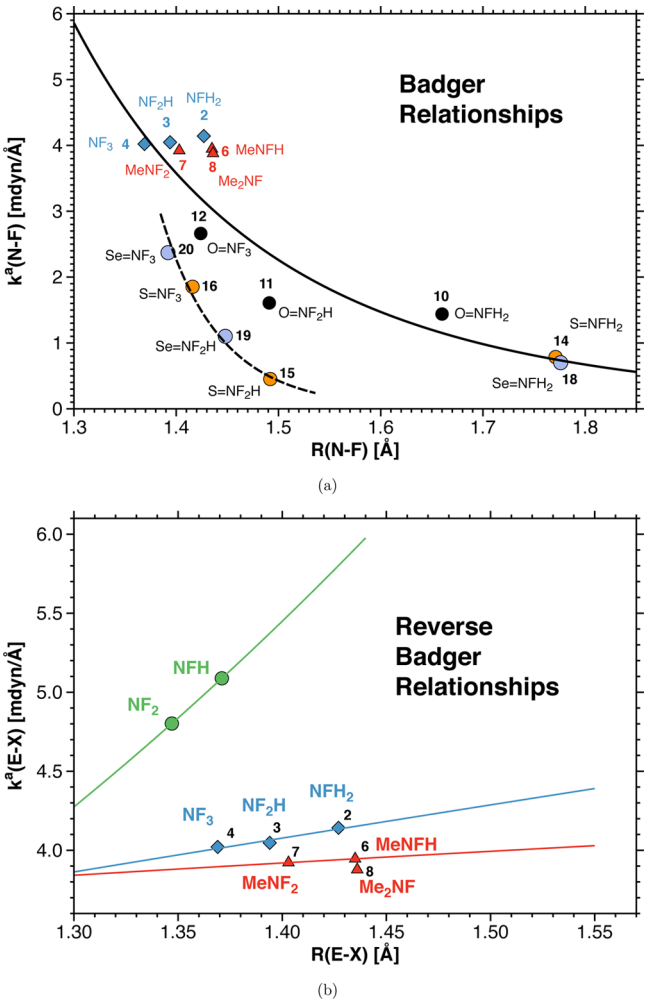

Figure 5. (a) Inverse BLBS relationships for all NF bonds investigated. (b) Reverse BLBS relationships in the cases of NF bond anomalies. CCSD(T)/aug-cc-pVTZ calculations.

have peculiar bond properties, which are difficult to describe by a Badger-type inverse BLBS relationship. Even if two or three BLBS relationships are used (solid and dashed lines in Figure 5a), the scattering of data points is large. It is more reasonable to consider different classes of fluoro amines separately as in Figure 5b (blue line, fluoro amines; red, methyl fluoro amines; green, fluoro amine radicals, which have been added for reasons of completeness). The N−F bonds of each of these fluoro amine classes follow a reverse BLBS relationship in line with a bond anomaly; that is, the CCSD(T) results confirm the previous (and current) DFT results (see Table 1).

Cremer and Kraka[13] explained the N−F bond anomaly as a result of bond shortening caused by increasing fluorination. Shorter N−F bonds are weakened by an increase in lp(N)−lp(F) repulsion. However, this explanation would imply that for the planar fluoro amines the NF anomaly increases, which is not the case. Therefore, a revised and more detailed explanation of the observed bond anomalies based on the calculated stretching force constants, bond lengths, and NBO charges is appropriate. Clearly, increasing fluorination leads to a strong withdrawal of negative charge from the N atom, which becomes highly positively charged (Figure 1). Its valence orbitals contract so that its covalent radius becomes smaller and the NF bonds become shorter. Pyramidalization of the planar molecular form of **1** is a consequence of the second order Jahn−Teller (SOJT) effect[96−99] involving the two a_1-symmetrical frontier orbitals. The highest occupied molecular orbital (HOMO) is dominated by the lp(N) orbital, whereas the antibonding (lowest unoccupied molecular orbital) LUMO has a dominant contribution from the substituents of N. The smaller the HOMO−LUMO gap is the stronger is the pyramidalization of the molecule as reflected by the pyramidalization angle θ. If the H atoms in **1** are replaced by F, the energy of the LUMO decreases thus closing the HOMO−LUMO gap and leading to a stronger pyramidalization (see red θ values in Figure 1). A stronger pyramidalization leads to increased p-orbital character of the bond orbitals (*hybridization defect*[100−105]) and a concomitant weakening of the NF bonds. This effect is enhanced by two lp−lp repulsion effects: (i) Through-space lp(F)−lp(F) repulsion between two or three F atoms in the pyramidal forms. (ii) Decreased anomeric delocalization of the lp(F) into a vicinal σ^*(NF) orbital. This is maximal for the planar form and the in-plane lp(F) electrons lowering in this way through-space lp−lp repulsion. For the pyramidal form, lp(F)−lp(F) repulsion also increases because anomeric lp(F) delocalization is strongly reduced.

This explanation model of the NF bond anomalies does not exclude that through-bond lp(N)−lp(F) repulsion also makes a bond weakening contribution. However, the latter cannot be decisive. Therefore, we will test in the following whether the conversion of the lp(N) into an NE bond (E = O, S, Se) leads to a vanishing of the N−F bond anomalies, which would attribute a decisive role to lp(N)−lp(F) repulsion.

Removal of the Nitrogen Lone Pair. If lp(N)−lp(F) repulsion in the fluoro amines would be the main cause for the observed bond anomalies, it would be eliminated when establishing an N→E (E = O, S, Se) donor−acceptor bond leading to $ONH_{3-n}F_n$, (n = 0, 1, ··· 3, **9**−**12**), $SNH_{3-n}F_n$ (**13**−**16**), and $SeNH_{3-n}F_n$, (**17**−**20**) so the NF bonds in these molecules should show a normal Badger-type behavior. On first sight, this seems to be the case although there are some unusual BLBS trends (Table 1; Figure 2): The NF bonds are significantly longer than in the corresponding fluoro amines, but decrease with increasing fluorination as found for the fluoro amines. This should lead to an increase in the bond strength, that is, a normal BLBS relationship should result. For the same number of F atoms, NF bond lengths increase from E = O to Se (n = 1) or decrease (n = 3; Figure 2). NE bond lengths decrease (E = O) or increase (E = Se) with fluorination or follow a mixed trend (E = S; first shortening, then lengthening, Figure 2). Bond anomalies are found for the NF and NS bonds of the pair **14**/**15**, which seems to be a consequence of the reversion of trends from the amine oxides to the amine selenides. The unusual NF bond lengths and ONF bond angles observed for **10**−**12** have been discussed in the literature.[106,107] MO theory suggests significant ionic contributions to bonding,[106] whereas the *Ligand Close Packing* model (a steric model) suggests predominantly covalent bonding.[107] The focus of this work is to elucidate the electronic structure changes taking place in the series **9**−**20** upon successive fluorination by

DOI: 10.1021/acs.jpca.5b05157
J. Phys. Chem. A 2015, 119, 9541−9556

utilizing local mode force constants k^a(NF) and k^a(NE) (E = O, S, Se) and NBO charges and to clarify what electronic effects lead to the overall trends in NF and NE bond lengths and the absence of the expected bond anomalies.

Because of the donor−acceptor bond N→O, the negative charge on N is reduced from −1022 me in **1** to −338 me in **9**, from −358 to +83 (**2**, **10**), +169 to +493 (**3**, **11**), and +561 to +802 me (**4**, **12**, Figure 1). Accordingly, the contraction of the covalent N radius should be stronger and the NF bonds shorter, which is not the case as they are significantly longer and weaker (Figure 5a). This is indicative of an anomeric effect involving the lp(O) electrons, which are delocalized into low-lying σ^*(NF) orbitals in the sense of a *back-donation mechanism* thus strengthening the NO bond, whereas the NF bonds are weakened. In **10**, the NO bond is 1.222 Å compared to 1.371 Å in **9** (0.149 Å reduction) and considerably stronger (k^a(NO) = 9.791 mdyn/Å. **9**: k^a(NO) = 4.102 mdyn/Å). The N−F bond becomes 0.223 Å longer than in **2** and significantly weaker as is reflected by the k^a(NF) value of 1.439 mdyn/Å compared to k^a(NF) = 4.142 mdyn/Å in **2**. The trends in the calculated R(NF) and k^a(NF) values suggest that the anomeric effect dominates the contraction effect thus leading in the amine oxides $ONH_{3-n}F_n$ always to weaker (longer) NF bonds.

We will show in the following that the absence of the lp(N) does not lead to a Badger-type inverse BLBS relationship and that anomeric delocalization involving the chalcogen lp disguises an existing NF bond anomaly partly. This requires a careful evaluation of the electronic effects determining the intrinsic strength of both the NF and NE bonds: (i) Anomeric delocalization will increase from O to S and Se because of the increase in the lp(E) energy. (ii) Also, it will increase with the number of F atoms in the NF_m group because this leads to a larger positive charge at N and lower lying $\sigma^*(NF_m)$ orbitals. (iii) However, with increasing m a strong impact on the NE bond will have just a $1/m$ fraction of this impact on an individual NF bond so that the anomeric NF bond lengthening should decrease with the number m of F atoms in the NF_m group. (iv) A large positive charge leads to a contraction of the N orbitals, which increasingly reduces the overlap with the lp(E) orbitals as they become more diffuse in the series O, S, Se.

In Figure 2, all relevant data needed to rationalize the various trends in the BLBS relations of **9**−**20** are summarized in which **9**, **13**, and **17** together with **2**−**4** serve as suitable reference molecules. Any shortening of the donor−acceptor bond NE upon fluorination indicates either contraction of the covalent radius of N or anomeric delocalization of lp(E) into the NF_m group. If there is a positive charge at E (Figure 2), anomeric delocalization should play an important role. With increasing positive charge at N, its lp orbital is contracted, which may lead to a shorter NE bond, but not necessarily to a stronger NE bond as the lp energy is reduced and the interaction with the np(E) orbital becomes energetically more difficult. On the basis of these general considerations the trends in the series 1−6 (brown outlined numbers) indicated in Figure 2 are shortly discussed.

Series 1: The decrease in the NE bond length (relative to the reference bond lengths: −0.149, −0.216, −0.216 Å) and increase in the NF bond lengths (0.233, 0.344, 0.349 Å) are predominantly caused by anomeric delocalization increasing from O to S and Se. *Series 4:* The increasing shortening of the NO bond length indicates increasing anomeric delocalization, which is facilitated by decreasing $\sigma^*(NF_m)$ orbital energies. As the anomeric delocalization effect is shared by an increasing number of NF bonds, individual NF bonds experience a reduction in bond lengthening so that shorter NF bonds result with increasing m. The intrinsic bond strength increases. Obviously, the anomeric effect outweighs through-space lp(F)−lp(F) repulsion and hybridization defects. However, Figure 5a reveals that both **11** and **12** have too low NF stretching force constants compared to **10** and that it is justified to speak of a *hidden bond anomaly*.

Series 2: The decrease of the NE bond length is partly stronger and partly weaker. Anomeric delocalization slightly increases for S, but then decreases because of a decrease in overlap between the 4pπ-orbital and the contracted $\sigma^*(NF_2)$ orbitals, which is revealed by a reduction of the NSe bond length by just 0.180 Å. Through-space lp−lp repulsion weakens the NF bonds. A NF bond anomaly results as is revealed by the positions of the **11**, **15**, and **19** data points in Figure 5a. *Series 5:* The intrinsic NS bond strength steadily decreases according to the CCSD(T) local NS force constants, which suggest a decrease in lp(S)−$\sigma^*(NF_m)$ orbital overlap and anomeric delocalization. The NE bond lengths (1.619, 1.608, 1.614 Å, Figure 2) indicate a bond anomaly, which can result from several effects: changes in the NS donor bond because of orbital contraction at N, through-space lp(S)−lp(F) repulsion, or hybridization defects. A bond anomaly is also found for the NF bonds: For **15**, the local NF force constant is unusually low k^a(NF) of **14**−**16**: 0.786, 0.452, 1.853 mdyn/Å, see Table 1; R(NF): 1.771, 1.492, 1.416 Å. Comparison with the corresponding values for reference molecules **2**−**4** clarifies that anomeric delocalization is still the dominant effect (NBO charges at S: +212, +153, +161 me). Figure 5a confirms that the irregularity of the NF bonds in series 5 is stronger than that in series 4, but that trends are similar.

Series 3: Because of the decrease in anomeric lp(E) delocalization from **12** to **20**, the NF bond length decreases, whereas the bond strength does not show the expected increase, which is in line with another bond anomaly. Especially the k^a(NF) value of **16** is unusually low (**12**, **16**, **20**: 2.662, 1.853, 2.371 mdyn/Å) thus confirming the impression that bonding in the $SNH_{3-n}F_n$ molecules is at the crossing point of different electronic effects (anomeric delocalization decreasing, the donor−acceptor bond decreasing, the covalent radius of N decreasing, through-space lp−lp repulsion increasing, hybridization defects increasing). It would be a misleading simplification to focus on one "dominating" effect in this case. *Series 6:* The anomeric delocalization effect is clearly weaker as for the O and S series 4 and 5 (reflected by the decreases in the NSe bond length: 0.216, 0.180, 0.159 Å). With increasing fluorination, there is another decrease of anomeric delocalization, which leads to a lengthening/weakening of the NSe bond and a shortening/strengthening of the NF bonds, thus indicating that the anomeric effect still dominates in this series (Figure 2).

Inspection of Figure 5a confirms that all $ENH_{3-n}F_n$ (E: O, S, Se) molecules possess an unusual BLBS behavior, which is reminiscent of the fluoro amines, but which is partly disguised by anomeric delocalization of the lp(E)→$\sigma^*(NF_m)$ type. Therefore, it is appropriate to speak of hidden bond anomalies and hidden reverse BLBS relationships. Clearly, through-bond lp(N)−lp(F) repulsion is not the reason for the N−F bond anomaly observed for the fluoro amines. The N−F bond anomalies are disguised by strong anomeric delocalization, which leads to some of the weakest NF bonds found so far with

DOI: 10.1021/acs.jpca.5b05157
J. Phys. Chem. A 2015, 119, 9541−9556

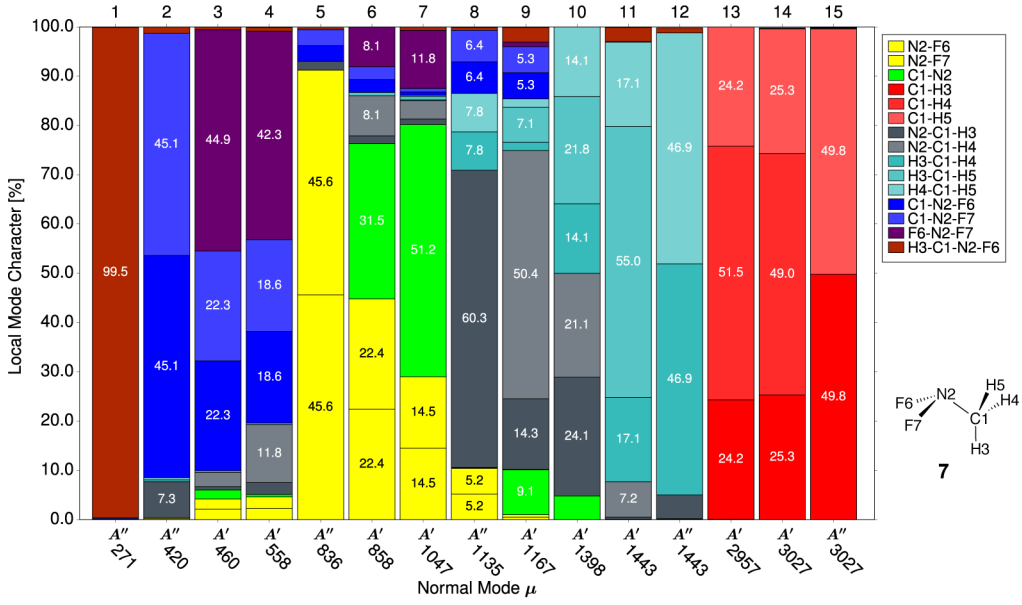

(a)

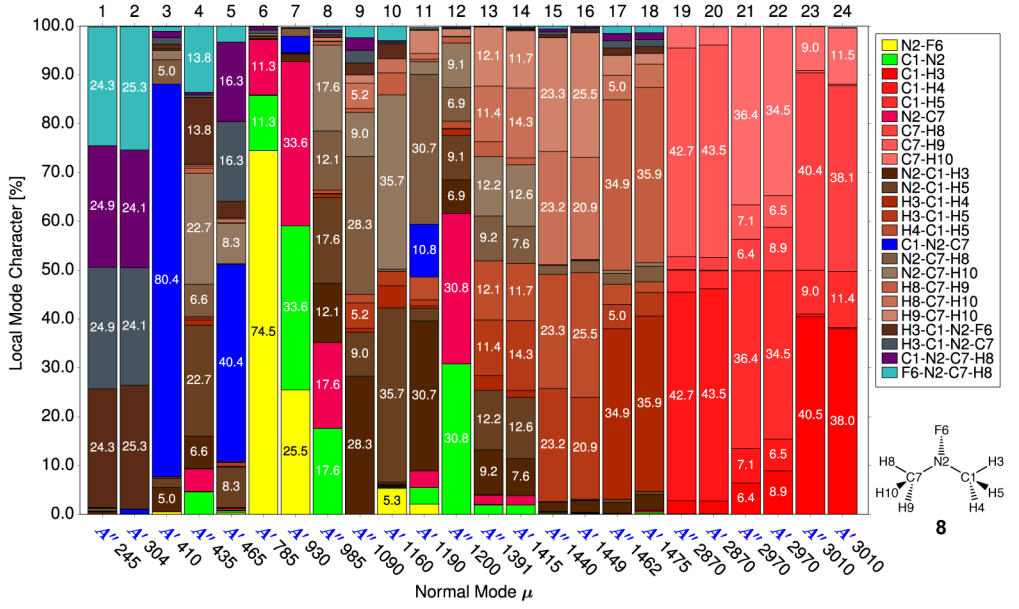

(b)

Figure 6. Decomposition of the (a) 15 normal vibrational modes of methyl difluoro amine (**7**) and (b) 24 normal modes of dimethyl fluoro amine (**8**) into local vibrational modes based on measured frequencies.[30] The color code (given on the right side) identifies each local mode and the internal coordinate driving it.[46] Each contribution is given in percentage. For the numbering of atoms, see the inset on the right side.

BSO values between 0.2 and 0.4 (amine sulfides **15** and **14**; amine selenides **18** and **19**; see Figure 4), which could be used as suitable fluorination agents.

Methyl Fluoro Amines. In methyl amine (**5**), the negative charge at N is decreased by 219 to −803 me with regard to ammonia (**1**) (Figure 1) primarily because the methyl group can get some of the negative charge σ-donated to N back via in-plane lp(N)−σ^*(CH) interactions as indicated by a C−H bond lengthening to 1.095 Å. In CH_3NHF (**6**) the negative charge on N is reduced by 594 to −209 me and in CH_3NF_2 (**7**) by 1057 to +254 me with regard to the parent molecules **2** and **3**, respectively. The change from **6** to **7** (463 me more positive N) is comparable to that found for the fluoro amines. Therefore, as shown in Figure 5a, the NF bonds in **6** (R(NF): 1.435 Å; k^a(NF): 3.946 mdyn/Å) and **7** (1.403 Å; 3.922 mdyn/Å) change according to a reverse BLBS relationship describing another NF bond anomaly. The effect is for a similar bond length decrease of 0.032 (0.033) Å four times smaller (Δk^a = 0.024 compared to 0.095 mdyn/Å), which is a result of the smaller charge at N and the larger covalent N radius caused by the hyperconjugative stabilization of the amine via its methyl group.

DOI: 10.1021/acs.jpca.5b05157
J. Phys. Chem. A 2015, 119, 9541−9556

Table 3. Normal Mode and Local Mode Properties for Methyl Difluoro Amine (7) Based on Experimental Frequencies[a]

		ω_μ			k^a	ω^a	ω_{coup}
μ	symbol	cm^{-1}	no.	internal coordinate	mdyn $Å^{-1}$	cm^{-1}	cm^{-1}
15	A''	3027	6	C1−H5	4.954	3007	20
14	A'	3027	4	C1−H3	4.954	3007	20
13	A'	2957	5	C1−H4	4.892	2989	−32
12	A''	1443	11	H4−C1−H5	0.633	1416	27
11	A'	1443	9	H3−C1−H4	0.633	1416	27
10	A'	1398	10	H3−C1−H5	0.627	1410	−12
9	A'	1167	7	N2−C1−H3	0.809	1179	−12
8	A''	1134	8	N2−C1−H4	0.798	1174	−40
7	A'	1047	3	C1−N2	3.979	1022	25
6	A'	858	2	N2−F7	3.686	881	−23
5	A''	836	1	N2−F6	3.686	881	−45
4	A'	558	14	F6−N2−F7	1.720	637	−79
3	A'	460	13	C1−N2−F7	1.393	599	−139
2	A''	420	12	C1−N2−F6	1.393	599	−179
1	A''	271	15	H3−C1−N2-F6	0.117	477	−206
ZPE [kcal/mol]:		28.66				29.59	−0.93

[a]Measured frequencies from ref 26 and 30. Local mode frequencies are characterized by the internal coordinate, which drives the mode. They are ordered according to the ACS, which relates each local mode to a particular normal mode. The coupling frequency ω_{coup} provides a measure of mode−mode coupling.[48,49,51] The zeropoint energy (ZPE) is calculated for each set of frequencies and leads to the value ZPE(normal) = ZPE(local) + ZPE(coup).

Table 4. Normal Mode and Local Mode Properties for Dimethyl Fluoro Amine (8) Based on Experimental Frequencies[a]

		ω_μ			k^a	ω^a	ω_{coup}
μ	sym	cm^{-1}	no.	internal coordinate	mdyn $Å^{-1}$	cm^{-1}	cm^{-1}
24	A'	3010	7	C7−H8	4.909	2994	16
23	A''	3010	3	C1−H3	4.909	2994	16
22	A'	2970	5	C1−H5	4.820	2966	4
21	A''	2970	9	C7−H10	4.820	2966	4
20	A'	2870	8	C7−H9	4.532	2876	−6
19	A''	2870	4	C1−H4	4.532	2876	−6
18	A'	1475	18	H8−C7−H9	0.665	1446	29
17	A''	1462	12	H3−C1−H4	0.665	1446	16
16	A'	1449	13	H3−C1−H5	0.636	1417	32
15	A''	1440	19	H8−C7−H10	0.636	1417	23
14	A'	1415	14	H4−C1−H5	0.640	1416	−1
13	A''	1391	20	H9−C7−H10	0.640	1416	−25
12	A''	1200	10	N2−C1−H3	0.827	1195	5
11	A'	1190	16	N2−C7−H8	0.827	1195	−5
10	A'	1160	17	N2−C7−H10	0.801	1171	−11
9	A''	1090	11	N2−C1−H5	0.801	1171	−81
8	A''	985	6	N2−C7	4.176	1047	−62
7	A'	930	2	C1−N2	4.176	1047	−117
6	A'	785	1	N2−F6	3.435	850	−65
5	A'	465	15	C1−N2−C7	1.116	573	−108
4	A''	435	21	H3−C1−N2-F6	0.119	488	−53
3	A'	410	24	F6−N2−C7-H8	0.119	488	−78
2	A'	304	23	C1−N2−C7-H8	0.116	467	−163
1	A''	245	22	H3−C1−N2-C7	0.116	467	−222
ZPE [kcal/mol]:		50.79				52.02	−1.23

[a]Measured frequencies from ref 28. Local mode frequencies are characterized by the internal coordinate, which drives the mode. They are ordered according to the ACS, which relates each local mode to a particular normal mode. The coupling frequency ω_{coup} provides a measure of mode−mode coupling.[48,49,51] The zeropoint energy (ZPE) is calculated for each set of frequencies and leads to the value ZPE(normal) = ZPE(local) + ZPE(coup).

Substitution of two hydrogens by methyl as in **8** (R(NF): 1.436 Å; k^a(NF): 3.878 mdyn/Å) leads to a normal effect, that is, an inverse BLBS relationship. Oberhammer and co-workers published the gas-phase structure of **8**.[27,28] They observed a

DOI: 10.1021/acs.jpca.5b05157
J. Phys. Chem. A 2015, 119, 9541−9556

bond length increase from 1.371 Å in **4**[108] to 1.447 Å in **8**. On the basis of a normal-mode analysis, they derived MP2/6-311++G(d,p) N−F stretching force constants of 4.58 and 4.77 mdyn/Å for **4** and **8**, respectively, which suggested a reverse BLBS relationship contrary to the CCSD(T) results obtained in this work: R(NF) of 1.369, 1.436 Å; $k^a(NF)$ of 4.021, 3.878 mdyn/Å (Table 1). Hagen and co-workers published the gas phase structure of difluoro methyl amine **7** and derived MP2 N−F stretching force constants for fluoro amines utilizing symmetry coordinates and scaling the results to fit observed infrared frequencies.[30] By assuming the symmetric NF stretching frequency to have a value of 1443 cm^{-1}, they derived NF force constants for **4**, **7**, and **8**, which supported an inverse BLBS relationship in line with Badger's rule.

In both publications, NF bonding is discussed on the basis of normal vibrational modes. However, normal vibrational modes are kinematically coupled and because of this it is erroneous to single out a normal mode as an NF stretching mode and use it to derive a local (pure) NF stretching force constant. The decomposition of the normal modes of **7** into local mode components (see Figure 6a, Table 3) using the experimental frequencies of Hagen and co-workers reveals that the characterization of frequency 11 at 1443 cm^{-1} as the NF stretching frequency is misleading. The symmetric and asymmetric normal modes 11 and 12 (both at ω_{11} = 1443 cm^{-1}) are admixtures of NCH and HCH bending vibrations. The normal modes with the highest NF character are the A''-symmetrical mode 5 (ω_5 = 836 cm^{-1}; 91% NF stretching +9% of HCH and NCH bending character) and the A''-symmetrical mode 6 (ω_6 = 858 cm^{-1}; 44% NF stretching + more than 30% CN stretching character). Normal modes 7 and 8 contain still 30% and 10% NF stretching character. Therefore, none of the force constants of these normal modes is qualified to serve as an unique NF bond strength descriptor. Instead, we derive from the experimental frequencies a local NF stretching frequency of ω^a(NF) = 881 cm^{-1}, which is associated with a local NF stretching force constant k^a(NF) of 3.683 mdyn/Å (Table 3). Even in the case of **8** with just one NF bond, there is no normal mode with pure NF character as is obvious from Figure 6b and Table 4. Normal mode 6 has 75% NF stretching character mixed with 25% CN stretching character.

Critical Assessment of Postulated Reverse BLBS Relationships. Reverse BLBS relationships have been reported for heavy metal bonds,[45] Ti bonds,[43,44] and transition metal hydrides.[42] We focus this work on the investigation of Pb−F and Pb−C single bonds in methylated lead molecules of the type $(CH_3)_nPb(II)F_{(2-n)}$ (n = 0−2, **33**−**35**) and $(CH_3)_nPb(IV)F_{(4-n)}$ (n = 0−4, **36**−**39**),[45] Ti−P bonds in $P(CH_3)_3$, $P(OC_2H_5)_3$, and PF_3 adducts of open titanocene, Ti(η^5-2,4-$C_7H_{11})_2$, (**40**−**42**),[43,44] and Cr−H bonds in chromium cyclopentadienyl hydrides **47**−**51**[42] (see Figure 3). Molecules **43**−**46**, **52**, and **53** are investigated to get the reference values needed in this connection.

The studies cited above used binding energies as bond strength descriptors (derived from NMR measurements) for the Ti−P bonds,[43,44] measured or quantum chemical BDE values for the Cr−H bonds,[42] and calculated relative stabilities derived from isodesmic reactions for the Pb−F and Pb−C bonds.[45] As discussed in the introduction, BDE (BDH) values are disqualified as measures for the intrinsic strength of a bond because they depend on the stability of the fragments generated, which are stabilized in different ways via geometry relaxation and electron density reorganization.[8] The same holds for binding energies and model based relative stabilities. Therefore, we have reevaluated the BLBS relationships for these molecules and have identified them as either inverse (Badger-type) or reverse BLBS relationships utilizing the local stretching force constant k^a as reliable bond strength descriptor.

Intrinsic Strength of Pb−F Bonds. Kaupp and Schleyer[45] reported that in $(R_nPb(II)FX_{(2-n)}$ (n = 0−2) and $(R_nPb(IV)FX_{(4-n)}$ (n = 0−4; R = H, CH_3; X = F, Cl) the Pb−R and Pb−X bonds shorten upon successive halogenation but seem to become weaker if the relative stabilities of the molecules in question are calculated.[45] They concluded that successive halogenation leads to an increase of the metal charge, followed by an increase of the difference in the radial extensions of the Pb 6s and 6p orbitals making sp^n hybridization less favorable and the covalent bonds in these compounds weaker. However, as discussed above, sp^n hybridization plays only a major role in the case of bonding between second row atoms and, therefore, it should not significantly influence the strength of bonds involving the heavy metal Pb. The increase of positive charge on Pb (Pb charges for the Pb(II) series: **33**, +1031; **34**, +1316; **35**, +1560. Pb charges for the Pb(IV) series: **36**, +1732; **37**, +2001; **38**, +2257; **39**, +2537 me; Figure 3) leads to a decrease of the Pb covalent radius and accordingly should imply shorter and stronger Pb bonds. This is reflected by the local mode force constants k^a in a quantitative way. We find Badger-type BLBS relationships for both Pb−C and Pb−F bonds (Figure 7a and 7b) with no sign of any bond anomalies. Obviously, intrinsic bond strengths cannot be reliably predicted using isodesmic or other model reactions, which always depend on the electronic structure changes in both reactants and products and do not characterize any specific bond.

Intrinsic Strength of Ti−P Bonds. Ernst and co-workers[43] discussed Ti(II) compounds **40**−**42** as examples for a reverse BLBS relationship. They determined Ti−P bond lengths of 2.550(2) (**40**), 2.472(4) (**41**), and 2.324(2) Å (**42**) by single crystal X-ray diffraction studies and used as measures for the Ti−P bond strength the following BDHs: 14.5(8) (**41**), 10.6(6) (**42**), and 17.4(8) kcal/mol (**43**) in which these values were derived from ^{13}P NMR spectra by monitoring the dissociation of the phosphine adducts in THF solution.[44] These BDH values led them to the conclusion that **42** has the shortest and strongest Ti−P bond in this series, whereas the BLBS order for **40** and **41** is reversed. Calculated local Ti−P stretching force constants do not confirm their assumption (see Table 2 and Figure 7). The R(TiP) and k^a(TiP) values of 2.521 Å and 0.940 mdyn/Å (**40**), 2.416 and 1.124 (**41**), and 2.293 and 1.753 (**42**) are in line with a normal BLBS relationship, which is also in line with the BDE (BDH) values calculated in this work: 13.0 (11.2) kcal/mol (**40**), 15.6 (13.6) (**41**), and 20.4 (18.0) (**42**).

As is revealed by an NBO analysis of complexes **40**−**42** and the corresponding monomers, that is, the open titanocene (**43**), the phosphines $P(Me_3)_3$ (**44**), $P(OEt)_3$ (**45**), and PF_3 (**46**), the Ti−P bond strength depends on the positive charge on P (red numbers in Figure 3). With increasing electronegativity of X in the series X = Me, OEt, F, the positive charge on P increases from +803 me in **44** to +1610 me in **45** and +1743 me in **46**. Upon complexation with **43**, the charge of the Me, OEt, and F substituent hardly changes, whereas the positive charge on P increases to +1184 (**40**), +2123 (**41**), and +2232 me (**42**). This is indicative of a charge transfer from P to Ti as is reflected by the charge on Ti which changes from +988 (**43**) to −72 (**72**). The positive charge on P leads to a contraction of its covalent

DOI: 10.1021/acs.jpca.5b05157
J. Phys. Chem. A 2015, 119, 9541−9556

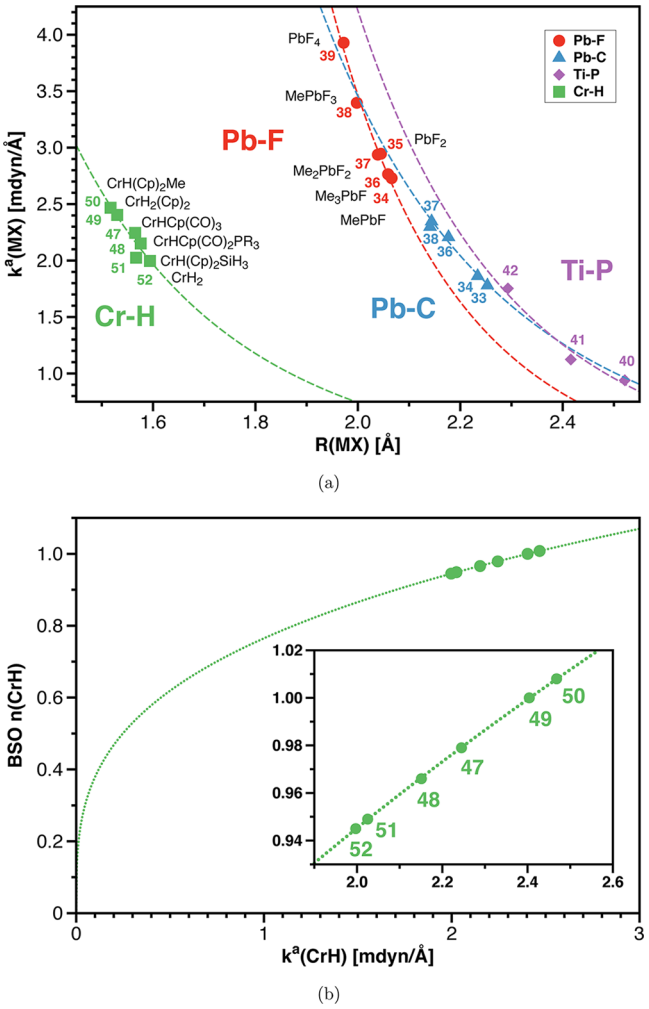

Figure 7. (a) Inverse Badger-type BLBS relationships between the bond length R and the local stretching force constant k^a of Ti−P (purple), Cr−H (green), Pb−C (blue), and Pb−F bonds (red). (b) Relative BSO values n(CrH) given as a function of the corresponding local stretching force constants. DFT calculations, see text.

radius. The orbital energy of the P lone pair decreases, increasing the overlap with one of the adjacent empty Ti d-orbitals thus supporting the charge transfer from P to Ti. As a result, the Ti−P bond becomes shorter and stronger where the intrinsic strength of the TiP bond depends on the amount of charge transfer and the overlap of the bonding orbitals.

Intrinsic Strength of Cr−H Bonds. Recently, Tang, Fu, and Guo reported a reverse BLBS relationship for Cr−H bonds in a series of 32 Cr hydrides.[42] They used experimental BDHs[14] as well as calculated BDEs (B3P86/LanL2DZ+P[77,109−111] calculations without BSSE corrections) as bond strength descriptors. In Table 2, local stretching force constants k^a(CrH) for a selection of the reported Cr hydrides are listed, including two chromium(IV)-cyclopentadienyl-hydrides, **47** and **48**, three Cr(II)-dicyclopentadienyl hydrides (**49**−**51**), and as reference molecules chromium dihydride (**52**) and chromocene (**53**).[112−120] In Figure 7, it is shown that force constants k^a(CrH) and CrH bond lengths R(CrH) (green curve) follow a Badger-type BLBS relationship. Although the variation in the Cr−H bond length includes only 0.1 Å, the large variation in the Cr charges (−2451 me in **48** to +621 me in **52**) and H charges (+324 in **50** to −310 me in **52**, see Figure 3 and Table 2) confirms that CrH bonding in very different electronic environments is investigated and, because of this, the inclusion of additional Cr-hydrides would not change our conclusion.

Molecule **50** has the strongest CrH bond with a BSO value of 1.008. The weakest CrH bond is found for the chromium dihydride **52** with a BSO value of 0.945. It is interesting to note that although the investigated chromium hydrides show a large variety of Cr and H charges with $Cr^{\delta-}$ $H^{\delta+}$ polarization, (**47**−**51**) and $Cr^{\delta+}$ $H^{\delta-}$ polarization (**52**) the spread in the BSO values is relatively small (Figure 7). A Cr−H bond anomaly cannot be expected because any destabilizing electronic factor upon bond shortening is absent. Since Cr hydrides play a key role in catalytic hydrogenation processes,[121,122] the quantitative assessment of the CrH bond strength as provided by the local stretching force constants can serve as an important design tool. An extensive study of CrH bonding based on the local vibrational mode analysis is in progress.

Basic Problems of Testing Badger-Type Relationships in Transition Metal Complexes. The Badger relationship between stretching force constants as descriptors for the intrinsic bond strength is originally derived for diatomic molecules[24,25] and the extended Badger relationship discussed in several recent studies[12,31,123] is qualitatively fulfilled for bonds with a similar bonding mechanism. The scattering of the (k^a,R) data points increases with an increasing variation in the bonding mechanism, for example, when the bonding for main group elements is compared with that for transition metal complexes or lanthanide and actinide molecules. With an increase in scattering, a reversion of the BLBS relationship becomes easily possible. We demonstrate this by focusing on the Ti complexes **40**−**43** and the Cr complexes **47**−**53** on the metal−carbon bonding with the 2,4-dimethyl-pentadienyl and cyclopentadienyl anion ligands, respectively, which is best accomplished by considering distance R(MX) and stretching force constant k^a(MX) for the interaction between M and the geometrical center X of the π-ligand. These values are also listed in Table 2.

For the Ti complexes **40**−**42** the R(MX) distance decreases from 1.756 to 1.743 Å, which leads to an increase of the k^a(MX) force constant from 0.941 to 1.301 mdyn/Å, in line with an inverse BLBS relation. The Ti complex **43** has an R(MX) value of 1.888 Å and a k^a(MX) value of 1.054 mdyn/Å (larger than that of **40**) and thereby violates the Badger-type relation for the other Ti complexes. These are 16-electron complexes, whereas **43** is a 14-electron complex, which has a different type of bonding as it is obvious from the calculated NBO charges at Ti summarized in Figure 3. The changes in bonding from one complex type to the other are interesting and can be discussed on the basis of the charge distribution and the intrinsic bond strengths; however, they do not necessarily indicate an anomaly in bonding as the bonding mechanism is different.

The situation is more complex in the Cr-hydrides **47**−**51**. According to the R(MX) and k^a(MX) values of Table 2, the two complexes **47** and **48** as well as chromocene (**53**) have unusual bonding situations as the R value is large (1.802 Å, but the k^a(MX) values (3.335 and 3.389 mdyn/Å) suggest stronger bonding interactions than those found for **50** or **53** (Table 2). Complexes **47**−**51** are all 18-electron complexes, whereas chromocene is a 16-electron complex, which has a different type of bonding. But even in the case of **47** and **48**, there is a bonding difference insofar as only one Cp-ligand is involved as compared to two Cp ligands in complexes **49**−**51**. The difference in the bonding mechanism is reflected by Cr charges

DOI: 10.1021/acs.jpca.5b05157
J. Phys. Chem. A 2015, 119, 9541−9556

of about −2.4 e in **47** and **48**, −1.1−1.5 e in **49** - **51**, and just 0.03 e in the case of **53**. An R(MX) value sensitively registers the changes in the charges of the connected centers, the atomic number of M, and other factors, whereas the local force constant k^a gives a reliable account of the intrinsic bond strength irrespective of the number of inner core−shells, the number of ligands, or the charge distribution. Therefore, it is inappropriate to compare Cr−Cp bonding in complexes with different bonding mechanisms and to speak of bond anomalies in these cases.

BDE Values as Bond Strength Descriptors. Since decades BDE values have been used to predict fragmentation patterns of molecules. In this connection, one speaks in a simplified way of the *strength of a bond* to resist fragmentation. BDE values include all changes taking place during the reaction as, for example, bond breaking, rehybridization, electron density reorganization, spin decoupling and recoupling effects, energy changes resulting from avoided crossings (diatomics), Jahn−Teller and pseudo-Jahn−Teller effects or changes in spin orbit coupling. The intrinsic bond strength does not include any of these effects as it refers to the strength of the bond in the equilibrium of the molecule and measured for an infinitesimal change of the bond. Therefore, it can be compared from molecule to molecule and reflects changes in the electronic structure of a molecule and its bonds even if they follow different dissociation mechanisms (e.g., homolytic vs heterolytic). Often intrinsic bond strength and reaction bond strength are mixed in discussions, which leads to erroneous conclusions.

The fact that calculated G4 BDE and BDH values are parallel in some cases to the intrinsic bond strength is misleading as the former parameters always depend on additional factors rather than just the strength of the bond being broken. As reaction energies they reflect also the stabilization of the dissociation products caused by a relaxation of electron density (major part) and geometry (minor part). These stabilization energies adopt large varying values, which in most cases disguise any trends in the intrinsic bond strength.[8,12,31] The fact that the calculated BDE and BDH values of the fluoro amines correctly reflect the NF bond anomaly only suggests that the relaxation mechanisms of the fragments are similar in these cases for the corresponding (fluoro)amine radicals. In recent work, we have given several examples revealing the shortcomings of BDE values as intrinsic bond strength descriptors.[8,12,60−62,68] This is also confirmed by the BDE values of the N−F bonds for the $SNH_{3-n}F_n$ molecules (Table 1).

4. CONCLUSIONS AND OUTLOOK

Bond anomalies lead to reverse (anti-Badger) rather than inverse, Badger-type BLBS relationships. They seem to be more frequent than it was thought in the form of either direct or hidden bond anomalies, in which an example of the former is given by the fluoro amines and one of the latter by the fluoro amine chalcogenides investigated in this work. Their detection requires reliable spectroscopic measurements or alternatively accurate quantum chemical calculations of the coupled cluster type if bonds between electronegative atoms are involved as in the case of the NF bond. Even more important is the evaluation of the intrinsic strength of a given bond, for which vibrational spectroscopy is the perfect, broadly applicable tool. It is always possible to convert normal into local vibrational modes using measured (e.g., the methyl fluoro amines) or calculated vibrational frequencies[13,31,46,47] as was confirmed in this work. In this way, the local stretching force constant of any bond can be determined, which as a dynamic parameter associated with an infinitesimal change in the bond length does not lead to any significant electronic structure changes, but probes the strength of the bond, and by this is the perfect descriptor of the intrinsic bond strength.

Utilizing CCSD(T) results for geometries, local stretching force constants, and NBO charges, bond anomalies have been confirmed for the fluoro amines, the methyl fluoro amines, and fluoro amine sulfides. They have been rationalized as an interplay of bond shortening and bond weakening effects in which the latter are a result of hybridization defects in connection with SOJT distortions, lp−lp repulsion, and anomeric lp delocalization. On the basis of the results of this work, bond anomalies and reverse BLBS relationships should be found for electron-rich bonds between second period or second period and third period atoms when considering equilibrium geometries.

The investigation of the fluorinated amine chalcogenides has established the existence of *hidden bond anomalies*, which result when a bond anomaly is disguised by another electronic effect. In the case of molecules **9**−**20** the mantling effect is an anomeric delocalization of the lp(E) electrons into the vicinal NF bonds thus shortening the NE and lengthening the NF bonds. Because the strength of anomeric delocalization can be assessed by the change in the NE bond length, it is possible to unravel the existence and magnitude of the underlying NF bond anomalies, which become an "open" anomaly for the amine sulfides because of two annihilating factors that determine the magnitude of anomeric delocalization. Through-bond lp(N)−lp(F) repulsion is less important than through-space lp(F)−lp(F) repulsion, which is a result of the large positive charge at N and a contraction of the lp(N) orbital in planar fluoro amines.

We have investigated three cases of claimed bond anomalies in connection with the Pb−C, Pb−F, Ti−P, or Cr−H bonds in molecules **33**−**53** and find for all these bonds a normal (inverse) Badger-type BLBS relationship; that is, the claimed bond anomalies do not exist. We also find that in none of these cases was a reliable intrinsic bond strength descriptor used in the previous investigations: BDEs or BDHs as well as the energies of isodesmic or other formal reactions are not suitable to reliably describe the intrinsic strength of a particular bond.

This work has also shown that reverse BLBS relationships can easily be found across the periodic table if one compares bonds, which are the result of very different bonding mechanisms. Therefore, we suggest that terms such as bond anomaly, anti-Badger behavior, or reverse BLBS relationships are exclusively used for those bonds that connect the same type of atoms according to the same type of bonding mechanism as in the case of the bonds studied in this work.

■ ASSOCIATED CONTENT

Supporting Information

The Supporting Information is available free of charge on the ACS Publications website at DOI: 10.1021/acs.jpca.5b05157.

Calculated geometries and energies for all molecules calculated in this work (PDF)

■ AUTHOR INFORMATION

Corresponding Author

*Tel.: 01-214-768-1300. E-mail: dcremer@smu.edu.

DOI: 10.1021/acs.jpca.5b05157
J. Phys. Chem. A 2015, 119, 9541−9556

Notes

The authors declare no competing financial interest.

■ ACKNOWLEDGMENTS

This work was financially supported by the National Science Foundation, Grant CHE 1464906. We thank SMU for providing computational resources.

■ REFERENCES

(1) Slater, J. C. Directed Valence in Polyatomic Molecules. *Phys. Rev.* **1931**, *37*, 481−497.
(2) Mulliken, R. S. Overlap Integrals and Chemical Binding. *J. Am. Chem. Soc.* **1950**, *72*, 4493−4503.
(3) Pauling, L. *The Nature of the Chemical Bond*; Cornell University Press: New York, 1960.
(4) McWeeny, R. *Coulson's Valence*; Oxford University Press: London, 1979.
(5) Frenking, G.; Shaik, S. *The Chemical Bond*; Wiley: 2014.
(6) Ruedenberg, K. The Physical Nature of the Chemical Bond. *Rev. Mod. Phys.* **1962**, *34*, 326−352.
(7) Kraka, E.; Cremer, D. In *Theoretical Models of Chemical Bonding. The Concept of the Chemical Bond*, Vol 2; Maksic, Z. B., Ed.; Springer Verlag, Heidelberg, 1990; pp 453−542.
(8) Cremer, D.; Wu, A.; Larsson, A.; Kraka, E. Some Thoughts about Bond Energies, Bond Lengths, and Force Constants. *J. Mol. Model.* **2000**, *6*, 396−412.
(9) Frenking, G., Shaik, S., Eds. *The Chemical Bond: Fundamental Aspects of Chemical Bonding*; Wiley: New York, 2014.
(10) Cremer, D.; Kraka, E. Theoretical Determination of Molecular Structure and Conformation. 15. Three-membered Rings: Bent Bonds, Ring Strain, and Surface Delocalization. *J. Am. Chem. Soc.* **1985**, *107*, 3800−3810.
(11) Kraka, E.; Cremer, D. In *Molecular Structure and Energetics, Structure and Reactivity*; Liebman, J. F., Greenberg, A., Eds.; VCH: Deerfield Beach, 1988; Vol. 7; pp 65−92.
(12) Kalescky, R.; Kraka, E.; Cremer, D. Identification of the Strongest Bonds in Chemistry. *J. Phys. Chem. A* **2013**, *117*, 8981−8995.
(13) Cremer, D.; Kraka, E. From Molecular Vibrations to Bonding, Chemical Reactions, and Reaction Mechanism. *Curr. Org. Chem.* **2010**, *14*, 1524−1560.
(14) Luo, Y.-R. *Comprehensive Handbook of Chemical Bond Energies*; Taylor and Francis: Boca Raton, FL, 2007.
(15) Cremer, D.; Gauss, J. Theoretical Determination of Molecular Structure and Conformation. 20. Re-evaluation of the Strain Energies of Cyclopropane and Cyclobutane - CC and CH Bond Energies, 1,3-Interactions, and σ-Aromaticity. *J. Am. Chem. Soc.* **1986**, *108*, 7467−7477.
(16) Bader, R. F. W. *Atoms in Molecules: A Quantum Theory, International Series of Monographs on Chemistry*; Oxford University Press: Oxford, 1995; Vol. 22.
(17) Bader, R. F. W.; Slee, T. S.; Cremer, D.; Kraka, E. Description of Conjugation and Hyperconjugation in Terms of Electron Distributions. *J. Am. Chem. Soc.* **1983**, *105*, 5061−5068.
(18) Gibbs, G. V.; Hill, F. C.; Boisen, M. B.; Downs, R. T. Power Law Relationships between Bond Length, Bond Strength and Electron Density Distributions. *Phys. Chem. Miner.* **1998**, *25*, 585−590.
(19) Gibbs, G. V.; Ross, N. L.; Cox, D. F.; Rosso, K. M.; Iversen, B. B.; Spackman, M. A. Pauling Bond Strength, Bond Length and Electron Density Distribution. *Phys. Chem. Miner.* **2014**, *41*, 17−25.
(20) Cremer, D.; Kraka, E. A Description of the Chemical Bond in Terms of Local Properties of Electron Density and Energy. *Croat. Chem. Acta* **1984**, *57*, 1259−1281.
(21) Cremer, D.; Kraka, E. Chemical Bonds without Bonding Electron Density - Does the Difference Electron Density Analysis Suffice for a Description of the Chemical Bond? *Angew. Chem., Int. Ed. Engl.* **1984**, *23*, 627−628.
(22) Wilson, E. B.; Decius, J. C.; Cross, P. C. *Molecular Vibrations. The Theory of Infrared and Raman Vibrational Spectra*; McGraw-Hill: New York, 1955.
(23) Woodward, L. A. *Introduction to the Theory of Molecular Vibrations and Vibrational Spectroscopy*; Oxford University Press: Oxford, 1972.
(24) Badger, R. M. A Relation between Internuclear Distances and Bond Force Constants. *J. Chem. Phys.* **1934**, *2*, 128−131.
(25) Badger, R. M. The Relation between the Internuclear Distances and Force Constants of Molecules and Its Application to Polyatomic Molecules. *J. Chem. Phys.* **1935**, *3*, 710−715.
(26) Atalla, R. H.; Craig, A. D.; Gailey, J. A. Infrared Spectrum of Methyldifluoramine. *J. Chem. Phys.* **1966**, *45*, 423−427.
(27) Mack, H.; Christen, D.; Oberhammer, H. J. Theoretical Study of Fluorinated Amines. *J. Mol. Struct.* **1988**, *190*, 215−226.
(28) Christen, D.; Gupta, O. D.; Kadel, J.; Kirchmeier, R. L.; Mack, H. G.; Oberhammer, H.; Shreeve, J. M. An Unusual Relationship between the N-F Bond Lengths and Force Constants in N-Fluoroamines. *J. Am. Chem. Soc.* **1991**, *113*, 9131−9135.
(29) Politzer, P.; Habibollahzadeh, D. Relationship between Dissociation Energies, Force Constants, and Bond Lengths for Some N-F And O-F Bonds. *J. Chem. Phys.* **1993**, *98*, 7659−7660.
(30) Hagen, K.; Hedberg, K.; John, E. O.; Robert, J.; Kirchmeier, L.; Shreeve, J. M. Structure and Vibrational Force Field of Methyldifluoroamine, CH_3NF_2. An Electron-diffraction Investigation Augmented by Microwave and Infrared Spectroscopic Data and by Ab Initio Molecular Orbital Calculations. *J. Phys. Chem. A* **1998**, *102*, 5106−5110.
(31) Kraka, E.; Larsson, J. A.; Cremer, D. In *Computational Spectroscopy: Methods, Experiments and Applications*; Grunenberg, J., Ed.; Wiley: New York, 2010; pp 105−149.
(32) Kaupp, M.; Metz, B.; Stoll, H. Breakdown of Bond Length-Bond Strength Correlation: A Case Study. *Angew. Chem., Int. Ed.* **2000**, *39*, 4607−4609.
(33) Kaupp, M.; Riedel, S. On the Lack of Correlation between Bond Lengths, Dissociation Energies, and Force Constants: The Fluorine-Substituted Ethane Homologues. *Inorg. Chim. Acta* **2004**, *357*, 1865−1872.
(34) Martell, J. M.; Boyd, R. J.; Shi, Z. Effects of Electron Correlation on the Series $C_2H_nF_{6-n}$ (n = 0−6): Geometries, Total Energies, and C-C and C-H Bond-Dissociation Energies. *J. Phys. Chem.* **1993**, *97*, 7208−7215.
(35) Pierce, L.; DiCianni, N.; Jackson, R. H. Centrifugal Distortion Effects in Asymmetric Rotor Molecules. I. Quadratic Potential Constants and Average Structure of Oxygen Difluoride from the Ground-state Rotational Spectrum. *J. Chem. Phys.* **1963**, *38*, 730−739.
(36) Kim, H.; Pearson, E.; Appelman, E. H. Millimeter-wave Spectrum and Structure of Hypofluorous Acid: HOF and DOF. *J. Chem. Phys.* **1972**, *56*, 1−3.
(37) Murrell, J.; Carter, S.; Mills, I. M.; Guest, M. F. Analytical Potentials for Triatomic Molecules from Spectroscopic Data. V. Application to HOX (X = F, Cl, Br, I). *Mol. Phys.* **1979**, *37*, 1199−1222.
(38) Ju, X.-H.; Wang, Z.-Y.; Yan, X.-F.; Xiao, H.-M. Density Functional Theory Studies on Dioxygen Difluoride and Other Fluorine/Oxygen Binary Compounds: Availability and Shortcoming. *J. Mol. Struct.: THEOCHEM* **2008**, *437*, 95−100.
(39) Harcourt, R.; Wolynec, P. Parametrized Valence Bond Studies of the Origin of the N-F Bond Lengthening of FNO_2 and FNO. *J. Phys. Chem. A* **2001**, *105*, 4974−4979.
(40) Lindquist, B. A.; Dunning, T. H. Bonding in $FSSF_3$: Breakdown in Bond Length-Strength Correlations and Implications for SF_2 Dimerization. *J. Phys. Chem. Lett.* **2013**, *4*, 3139−3143.
(41) Mueck, L. Bonding Analysis; United They are Strong. *Nat. Chem.* **2013**, *5*, 896−896.
(42) Tang, S.; Fu, Y.; Guo, Q. Ab Initio Calculation of M-H Bond Dissociation Energies of Cr-Group Metal Hydrides. *Huaxue Xuebao* **2012**, *70*, 1923−1929.

DOI: 10.1021/acs.jpca.5b05157
J. Phys. Chem. A 2015, 119, 9541−9556

(43) Ernst, R. D.; Freeman, J. W.; Stahl, L.; Wilson, D. R.; Arif, A. M.; Nuber, B.; Ziegler, M. L. Longer but Stronger Bonds: Structures of PF_3, $P(OEt)_3$, and PMe_3 Adducts of an Open Titanocene. *J. Am. Chem. Soc.* **1995**, *117*, 5075−5081.
(44) Stahl, L.; Ernst, R. Equilibria Studies Involving Ligand Coordination to "Open Titanocences": Phospine and Pentadienyl Cone Angle Influences and the Existence of These Electron-Deficient Molecules. *J. Am. Chem. Soc.* **1987**, *109*, 5673−5680.
(45) Kaupp, M.; Schleyer, P. v. R. Ab Initio Study of Structures and Stabilities of Substituted Lead Compounds - Why Is Inorganic Lead Chemistry Dominated by Pb(II) but Organolead Chemistry by Pb(IV). *J. Am. Chem. Soc.* **1993**, *115*, 1061−1073.
(46) Konkoli, Z.; Cremer, D. A New Way of Analyzing Vibrational Spectra. I. Derivation of Adiabatic Internal Modes. *Int. J. Quantum Chem.* **1998**, *67*, 1−9.
(47) Cremer, D.; Larsson, J. A.; Kraka, E. In *Theoretical Organic Chemistry*, Theoretical and Computational Chemistry; *Vol. 5*, Parkanyi, C., Ed.; Elsevier: Amsterdam, 1998; PP 259−327.
(48) Zou, W.; Kalescky, R.; Kraka, E.; Cremer, D. Relating Normal Vibrational Modes to Local Vibrational Modes with the Help of an Adiabatic Connection Scheme. *J. Chem. Phys.* **2012**, *137*, 084114.
(49) Zou, W.; Kalescky, R.; Kraka, E.; Cremer, D. Relating Normal Vibrational Modes to Local Vibrational Modes: Benzene and Naphthalene. *J. Mol. Model.* **2013**, *19*, 2865−2877.
(50) Zou, W.; Cremer, D. Properties of Local Vibrational Modes: The Infrared Intensity. *Theor. Chem. Acc.* **2014**, *133*, 1451−1−15.
(51) Kalescky, R.; Zou, W.; Kraka, E.; Cremer, D. Local Vibrational Modes of the Water Dimer - Comparison of Theory and Experiment. *Chem. Phys. Lett.* **2012**, *554*, 243−247.
(52) Kalescky, R.; Kraka, E.; Cremer, D. Local Vibrational Modes of the Formic Acid Dimer - The Strength of the Double Hydrogen Bond. *Mol. Phys.* **2013**, *111*, 1497−1510.
(53) McKean, D. C. Individual CH Bond Strengths in Simple Organic Compounds: Effects of Conformation and Substitution. *Chem. Soc. Rev.* **1978**, *7*, 399−422.
(54) Duncan, J. L.; Harvie, J. L.; McKean, D. C.; Cradock, C. The Ground State Structures of Disilane, Methyl Silane and the Silyl Halides, and an SiH Bond Length Correlation with Stretching Frequency. *J. Mol. Struct.* **1986**, *145*, 225−242.
(55) Murphy, W. F.; Zerbetto, F.; Duncan, J. L.; McKean, D. C. Vibrational Spectrum and Harmonic Force Field of Trimethylamine. *J. Phys. Chem.* **1993**, *97*, 581−595.
(56) Henry, B. R. The Local Mode Model and Overtone Spectra: A Probe of Molecular Structure and Conformation. *Acc. Chem. Res.* **1987**, *20*, 429−435.
(57) Kalescky, R.; Kraka, E.; Cremer, D. Description of Aromaticity with the Help of Vibrational Spectroscopy: Anthracene and Phenanthrene. *J. Phys. Chem. A* **2014**, *118*, 223−237.
(58) Humason, A.; Zou, W.; Cremer, D. 11,11-Dimethyl-1,6-methano[10]annulene - An Annulene with an Ultralong CC Bond or a Fluxional Molecule? *J. Phys. Chem. A* **2015**, *119*, 1666−1682.
(59) Kalescky, R.; Kraka, E.; Cremer, D. A New Approach to Tolman's Electronic Parameter Based on Local Vibrational Modes. *Inorg. Chem.* **2014**, *53*, 478−495.
(60) Kraka, E.; Cremer, D. Characterization of CF Bonds with Multiple-Bond Character: Bond Lengths, Stretching Force Constants, and Bond Dissociation Energies. *ChemPhysChem* **2009**, *10*, 686−698.
(61) Kalescky, R.; Kraka, E.; Cremer, D. Are Carbon-Halogen Double and Triple Bonds Possible? *Int. J. Quantum Chem.* **2014**, *114*, 1060−1072.
(62) Kalescky, R.; Zou, W.; Kraka, E.; Cremer, D. Quantitative Assessment of the Multiplicity of Carbon-Halogen Bonds: Carbenium and Halonium Ions with F, Cl, Br, I. *J. Phys. Chem. A* **2014**, *118*, 1948−1963.
(63) Oomens, J.; Kraka, E.; Nguyen, M.; Morton, T. Structure, Vibrational Spectra, and Unimolecular Dissociation of Gaseous 1-Fluoro-1-phenethyl Cations. *J. Phys. Chem. A* **2008**, *112*, 10774−10783.
(64) Kraka, E.; Cremer, D. Characterization of CF Bonds with Multiple-bond Character: Bond Lengths, Stretching Force Constants, and Bond Dissociation Energies. *ChemPhysChem* **2009**, *10*, 686−698.
(65) Freindorf, M.; Kraka, E.; Cremer, D. A Comprehensive Analysis of Hydrogen Bond Interactions Based on Local Vibrational Modes. *Int. J. Quantum Chem.* **2012**, *112*, 3174−3187.
(66) Kraka, E.; Freindorf, M.; Cremer, D. Chiral Discrimination by Vibrational Spectroscopy Utilizing Local Modes. *Chirality* **2013**, *25*, 185−196.
(67) Setiawan, D.; Kraka, E.; Cremer, D. Description of Pnicogen Bonding with the Help of Vibrational Spectroscopy - The Missing Link between Theory and Experiment. *Chem. Phys. Lett.* **2014**, *614*, 136−142.
(68) Setiawan, D.; Kraka, E.; Cremer, D. Strength of the Pnicogen Bond in Complexes Involving Group Va Elements N, P, and As. *J. Phys. Chem. A* **2015**, *119*, 1642−1656.
(69) Kalescky, R.; Zou, W.; Kraka, E.; Cremer, D. Vibrational Properties of the Isotopomers of the Water Dimer Derived from Experiment and Computations. *Aust. J. Chem.* **2014**, *67*, 426−434.
(70) Konkoli, Z.; Cremer, D. A New Way of Analyzing Vibrational Spectra. III. Characterization of Normal Vibrational Modes in Terms of Internal Vibrational Modes. *Int. J. Quantum Chem.* **1998**, *67*, 29−40.
(71) Raghavachari, K.; Trucks, G. W.; Pople, J. A.; Head-Gordon, M. A Fifth-order Perturbation Comparison of Electron Correlation Theories. *Chem. Phys. Lett.* **1989**, *157*, 479−483.
(72) Woon, D.; Dunning, T. J. Gaussian Basis Sets for Use in Correlated Molecular Calculations. IV. Calculation of Static Electrical Response Properties. *J. Chem. Phys.* **1994**, *100*, 2975−2988.
(73) Woon, D.; Dunning, T. Gaussian Basis Sets for Use in Correlated Molecular Calculations. III. The Atoms Aluminum Through Argon. *J. Chem. Phys.* **1993**, *98*, 1358−1371.
(74) Wilson, A.; Woon, D.; Peterson, K.; Dunning, T. Gaussian Basis Sets for Use in Correlated Molecular Calculations. IX. The Atoms Gallium through Krypton. *J. Chem. Phys.* **1999**, *110*, 7667−7676.
(75) Becke, A. D. Density-Functional Exchange-Energy Approximation with Correct Asymptotic Behavior. *Phys. Rev. A: At., Mol., Opt. Phys.* **1988**, *A38*, 3098−3100.
(76) Lee, C.; Yang, W.; Parr, R. G. Development of the Colle-Salvetti Correlation-Energy Formula into a Functional of the Electron Density. *Phys. Rev. B: Condens. Matter Mater. Phys.* **1988**, *B37*, 785−789.
(77) Becke, A. D. Density Functional Thermochemistry. III. The Role of Exact Exchange. *J. Chem. Phys.* **1993**, *98*, 5648−5652.
(78) Stephens, P. J.; Devlin, F. J.; Chabalowski, C. F.; Frisch, M. J. Ab Initio Calculation of Vibrational Absorption and Circular Dichroism Spectra Using Density Functional Force Fields. *J. Phys. Chem.* **1994**, *98*, 11623−11627.
(79) Vydrov, O. A.; Scuseria, G. E. Assessment of a Long Range Corrected Hybrid Functional. *J. Chem. Phys.* **2006**, *125*, 234109.
(80) Vydrov, O. A.; Heyd, J.; Krukau, A.; Scuseria, G. E. Importance of Short-range Versus Long-range Hartree-Fock Exchange for the Performance of Hybrid Density Functionals. *J. Chem. Phys.* **2006**, *125*, 074106.
(81) Vydrov, O. A.; Scuseria, G. E.; Perdew, J. P. Tests of Functionals for Systems with Fractional Electron Number. *J. Chem. Phys.* **2007**, *126*, 154109.
(82) Hariharan, P.; Pople, J. Influence of Polarization Functions on MO Hydrogenation Energies. *Theor. Chim. Acta* **1973**, *28*, 213−222.
(83) Clark, T.; Chandrasekhar, J.; Spitznagel, G. W.; Schleyer, P. v. R. Efficient Diffuse Function-Augmented Basis Sets for Anion Calculations. III. The 3-21+G Basis Set for First-Row Elements, Li-F. *J. Comput. Chem.* **1983**, *4*, 294−301.
(84) Peterson, K. A. Systematically Convergent Basis Sets with Relativistic Pseudopotentials. I. Correlation Consistent Basis Sets for The Post-d Group 13−15 Elements. *J. Chem. Phys.* **2003**, *119*, 11099.
(85) Peterson, K. A.; Figgen, D.; Goll, E.; Stoll, H.; Dolg, M. Systematically Convergent Basis Sets with Relativistic Pseudopotentials. II. Small-core Pseudopotentials and Correlation Consistent Basis Sets for the Post-d Group 16−18 Elements. *J. Chem. Phys.* **2003**, *119*, 11113.

DOI: 10.1021/acs.jpca.5b05157
J. Phys. Chem. A 2015, 119, 9541−9556

(86) Lebedev, V. I.; Skorokhodov, L. Quadrature Formulas of Orders 41, 47 and 53 for the Sphere. *Russian Acad. Sci. Dokl. Math.* **1992**, *45*, 587−592.
(87) Gräfenstein, J.; Cremer, D. Efficient DFT Integrations by Locally Augmented Radial Grids. *J. Chem. Phys.* **2007**, *127*, 164113.
(88) Curtiss, L. A.; Redfern, P. C.; Raghavachari, K. Gaussian-4 Theory. *J. Chem. Phys.* **2007**, *126*, 084108.
(89) Boys, S.; Bernardi, F. The Calculation of Small Molecular Interactions by the Differences of Separate Total Energies. Some Procedures with Reduced Errors. *Mol. Phys.* **1970**, *19*, 553−566.
(90) Reed, A.; Curtiss, L.; Weinhold, F. Intermolecular Interactions from a Natural Bond Orbital, Donor-Acceptor Viewpoint. *Chem. Rev.* **1988**, *88*, 899−926.
(91) Weinhold, F.; Landis, C. R. *Valency and Bonding: A Natural Bond Orbital Donor-Acceptor Perspective*; Cambridge University Press: 2003.
(92) Kraka, E.; Zou, W.; Filatov, M.; Gräfenstein, J.; Gauss, J.; He, Y.; Wu, A.; Konkoli, Z.; He, Z.; Cremer, D. et al. *COLOGNE15*; Southern Methodist University: Dallas, TX, 2015.
(93) Stanton, J. F.; Gauss, J.; Harding, M. E.; Szalay, P. G. CFOUR. 2010; see http//www.cfour.de (accessed 05-29-2015).
(94) Harding, M.; Metzroth, T.; Gauss, J.; Auer, A. Parallel Calculation of CCSD and CCSD(T) Analytic First and Second Derivatives. *J. Chem. Theory Comput.* **2008**, *4*, 64−74.
(95) Frisch, M.; Trucks, G. W.; Schlegel, H. B.; Scuseria, G. E.; Robb, M. A.; Cheeseman, J. R.; Scalmani, G.; Barone, V.; Mennucci, B.; Petersson, G. A. et al. *Gaussian 09* revision D.01; Gaussian Inc.: Wallingford CT, 2009.
(96) Opik, U.; Pryce, M. H. L. Studies of the Jahn-Teller Effect. I. A Survey of the Static Problem. *Proc. R. Soc. London, Ser. A* **1957**, *238*, 425−447.
(97) Bader, R. F. W. Vibrationally Induced Perturbations in Molecular Electron Distributions. *Can. J. Chem.* **1962**, *40*, 1164−1175.
(98) Pearson, R. G. The Second-Order Jahn-Teller Effect. *J. Mol. Struct.: THEOCHEM* **1983**, *103*, 25−34.
(99) Albright, T. A.; Burdett, J. K.; Whangbo, M.-H. *Orbital Interactions in Chemistry*; Wiley: New York, 2013.
(100) Kutzelnigg, W. Chemical Bonding in Higher Main Group Elements. *Angew. Chem., Int. Ed. Engl.* **1984**, *23*, 272−295.
(101) Kutzelnigg, W. Orthogonal and non-Orthogonal Hybrids. *J. Mol. Struct.: THEOCHEM* **1988**, *169*, 403−419.
(102) Pyykö, P. Dirac-Fock One-Centre Calculations Part 8. The $^1\Sigma$ States of ScH, YH, LaH, AcH, TmH, LuH and LrH. *Phys. Scr.* **1979**, *20*, 647−651.
(103) Pyykö, P. On the Interpretation of "Secondary Periodicity" in the Periodic System. *J. Chem. Res. Synop.* **1979**, 380−381.
(104) Kaupp, M. The Role of Radial Nodes of Atomic Orbitals for Chemical Bonding and the Periodic Table. *J. Comput. Chem.* **2007**, *28*, 320−325.
(105) Bartell, L. A Structural Chemist's Entanglement with Gillespie's Theories of Molecular Geometry. *Coord. Chem. Rev.* **2000**, *197*, 37−49.
(106) Tyrrell, J. Use of Oxidation-State Differences and Molecular Orbitals to Interpret Bonding in the Series ONXYZ (X, Y, Z = H, F, Cl), $HNNX_3$, $HNNX_2Y$, and $HNNXY_2$ (X, Y = H, F) and OCX_3^-, OCX_2Y^-, and $OCXY_2^-$ (X, Y = H, F). *J. Phys. Chem. A* **2006**, *110*, 228−233.
(107) Robinson, E. A.; Gillespie, R. J. Ligand Close Packing and the Geometry of the Fluorides of the Nonmetals of Periods 3, 4, and 5. *Inorg. Chem.* **2003**, *42*, 3865−3872.
(108) Sheridan, J.; Gordy, W. The Nuclear Quadrupole Moment of N^{14} and the Structure of Nitrogen Trifluoride from Microwave Spectra. *Phys. Rev.* **1950**, *79*, 513.
(109) Perdew, J. P. Density Functional Approximation for the Correlation Energy of the Inhomogeneous Electron Gas. *Phys. Rev. B: Condens. Matter Mater. Phys.* **1986**, *33*, 8822−8824.
(110) Wadt, W. R.; Hay, P. J. Ab Initio Effective Core Potentials for Molecular Calculations - Potentials for Main Group Elements Na to Bi. *J. Chem. Phys.* **1985**, *82*, 284−298.
(111) Hay, P. J.; Wadt, W. R. Ab initio Effective Core Potentials for Molecular Calculations - Potentials for K to Au Including the Outermost Core Orbitals. *J. Chem. Phys.* **1985**, *82*, 299−310.
(112) Pearson, R. The Transition Metal Hydrogen Bond. *Chem. Rev.* **1985**, *85*, 41−49.
(113) Estephane, J.; Groppo, E.; Vitillo, J. G.; Damin, A.; Gianolio, D.; Lamberti, C.; Bordiga, S.; Quadrelli, E. A.; Basset, J. M.; Kervern, G.; et al. A Multitechnique Approach to Spin-Flips for $Cp_2Cr(II)$ Chemistry in Confined State. *J. Phys. Chem. C* **2010**, *114*, 4451−4458.
(114) Xu, Z.-F.; Xie, Y.; Feng, W.-L.; Schaefer, H. F. Systematic Investigation of Electronic and Molecular Structures for the First Transition Metal Series Metallocenes $M(C_5H_5)_2$ (M= V, Cr, Mn, Fe, Co, and Ni). *J. Phys. Chem. A* **2003**, *107*, 2716−2729.
(115) Ma, B.; Collins, C. L.; Schaefer, H. F. Periodic Trends for Transition Metal Dihydrides MH_2, Dihydride Dihydrogen Complexes $MH_2\dot{H}_2$, and Tetrahydrides MH_4 (M= Ti, V, and Cr). *J. Am. Chem. Soc.* **1996**, *118*, 870−879.
(116) Ellis, J. E. Adventures with Substances Containing Metals in Negative Oxidation States. *Inorg. Chem.* **2006**, *45*, 3167−3186.
(117) Werner, H. *Landmarks in Organo-Transition Metal Chemistry: A Personal View*; Springer: New York, 2009.
(118) Haiduc, I.; Zuckerman, J. J. *Basic Organometallic Chemistry: Containing Comprehensive Bibliography*; Walter de Gruyter: Berlin, 1985.
(119) Smith, D. M.; Pulling, M. E.; Norton, J. R. Tin-Free and Catalytic Radical Cyclizations. *J. Am. Chem. Soc.* **2007**, *129*, 770−771.
(120) Norton, J. R.; Spataru, T.; Camaioni, D. M.; Lee, S.-J.; Li, G.; Choi, J.-W.; Franz, J. A. Kinetics and Mechanism of the Hydrogenation of the $CpCr(CO)_3\cdot/[CpCr(CO)_3]_2$ Equilibrium to $CpCr(CO)_3H$. *Organometallics* **2014**, *33*, 2496−2502.
(121) Crabtree, R. Dihydrogen Complexes: Some Structural and Chemical Studies. *Acc. Chem. Res.* **1990**, *23*, 95−101.
(122) Heinekey, D.; Oldham, W. Coordination Chemistry of Dihydrogen. *Chem. Rev.* **1993**, *93*, 913−926.
(123) Kurita, E.; Matsuura, H.; Ohno, K. Relationship between Force Constants and Bond Lengths for CX (X = C, Si, Ge, N, P, As, O, S, Se, F, Cl, And Br) Single and Multiple Bonds: Formulation of Badger's Rule for Universal Use. *Spectrochim. Acta, Part A* **2004**, *60*, 3013−3023.

DOI: 10.1021/acs.jpca.5b05157
J. Phys. Chem. A 2015, 119, 9541−9556